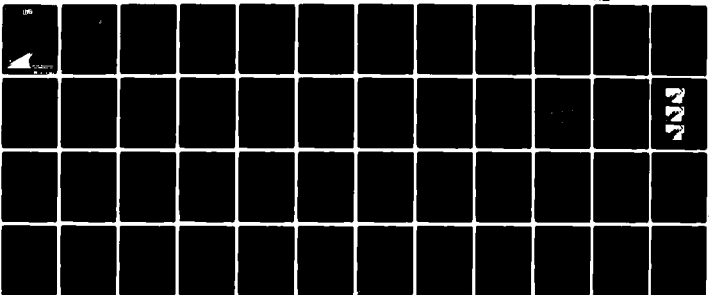
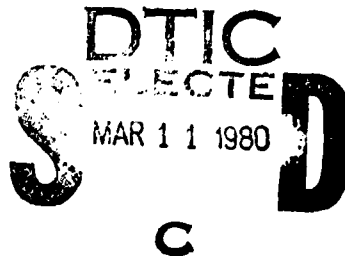


AD-A081 648 NIELSEN ENGINEERING AND RESEARCH INC MOUNTAIN VIEW CALIF F/6 20/4
ACTIVE CONTROL OF ASYMMETRIC VORTEX EFFECTS.(U)
DEC 79 J E FIDLER N60921-78-C-0073
UNCLASSIFIED NEAR-TR-212 NL

[OF]
20
AD-A081 648



END
DATE
FILMED
4-80
DTIC



ACTIVE CONTROL OF ASYMMETRIC VORTEX EFFECTS

BY

JOHN E. FIDLER
NIELSEN ENGINEERING & RESEARCH, INC.
510 CLYDE AVENUE
MOUNTAIN VIEW, CA 94043

DECEMBER 1979

FINAL REPORT FOR PERIOD 20 APRIL 1978 - 20 DECEMBER 1979

Approved for public release; distribution unlimited.

PREPARED FOR
NAVAL AIR SYSTEMS COMMAND
AIR-320C
WASHINGTON, DC 20361

NAVAL SURFACE WEAPONS CENTER
WHITE OAK
SILVER SPRING, MD 20910

Unclassified

SECURITY CLASSIFICATION OF THIS PAGE (When Data Entered)

REPORT DOCUMENTATION PAGE		READ INSTRUCTIONS BEFORE COMPLETING FORM
1. REPORT NUMBER 6 9 Final technical	2. GOVT ACCESSION NO.	3. RECIPIENT'S CATALOG NUMBER Apr 78 - 20 Dec 79
4. TITLE (and Subtitle) ACTIVE CONTROL OF ASYMMETRIC VORTEX EFFECTS		5. TYPE OF REPORT & PERIOD COVERED Final Technical Report 4/20/78 - 12/20/79
7. AUTHOR 10 John E. Fidler		6. PERFORMING ORG. REPORT NUMBER 14 NEAR-TR-212
		8. CONTRACT OR GRANT NUMBER(s) 15 N60921-78-C-0073
9. PERFORMING ORGANIZATION NAME AND ADDRESS Nielsen Engineering & Research, Inc. 510 Clyde Avenue Mountain View, CA 94043		10. PROGRAM ELEMENT, PROJECT, TASK AREA & WORK UNIT NUMBERS 61153N; 0; WR02-303-003; 0.
11. CONTROLLING OFFICE NAME AND ADDRESS Naval Air Systems Command AIR-320C Washington, DC 20361		12. REPORT DATE 11 December 1979
14. MONITORING AGENCY NAME & ADDRESS (if different from Controlling Office) Naval Surface Weapons Center White Oak Silver Spring, MD 20910 Attn: Code CK-81		13. NUMBER OF PAGES
		15. SECURITY CLASS. (of this report) Unclassified
		15a. DECLASSIFICATION/DOWNGRADING SCHEDULE
16. DISTRIBUTION STATEMENT (of this Report) 16 WK 2303 Approved for public release; distribution unlimited 17 NT 2303		
17. DISTRIBUTION STATEMENT (of this abstract entered in Block 20, if different from Report)		
18. SUPPLEMENTARY NOTES		
19. KEY WORDS (Continue on reverse side if necessary and identify by block number) Aerodynamics Aircraft High Angle of Attack Wind Tunnel Tests Vortices Missiles		
20. ABSTRACT (Continue on reverse side if necessary and identify by block number) Active control of asymmetric vortex effects on a pointed, slender body at high angles of attack has been achieved by rotating portions of the body about the axis. The lee side asymmetric vortex patterns and their associated yaw-plane forces and moments have been varied in cyclic, repeatable fashion at rates up to 100 cycles per second. The variations occurred so rapidly that the average yaw-plane quantities were brought to small, steady values.		

DD FORM 1 JAN 73 1473

389 724

Unclassified

SECURITY CLASSIFICATION OF THIS PAGE (When Data Entered)

Unclassified

SECURITY CLASSIFICATION OF THIS PAGE(When Data Entered)

20. Continued

or nulled out. The effect was obtained by rotating the nose, the nosetip and a band of the body surface just aft of the nose.



Unclassified

SECURITY CLASSIFICATION OF THIS PAGE(When Data Entered)

SUMMARY

An investigation has been conducted into the control of asymmetric vortex effects on a slender body. By means of spinning the nose, nosetip, and a band of the body surface just aft of the nose, the asymmetric vortex patterns and their effects have been alleviated and reduced. In particular, the problems due to the unpredictable magnitudes and directions of the induced yaw forces and moments have been removed. The spinning devices were rotated at speeds up to 100 rev/sec in the clockwise and counterclockwise directions. The tests were run at Mach numbers from 0.25 to 0.85 and angles of attack from 30° to 58°. The cyclic variations in out-of-plane forces and moments were found to be repeatable. It appeared that the body flow pattern could change more rapidly than could the vortex effects. Force, moment, hot wire, and flow visualization data are presented.

Accession For	
NTIS GRA&I	
DSC TAB	
Unannounced	
Justification	
By	
Distribution/	
Availability Codes	
Dist.	Avail and/or special
A	

TABLE OF CONTENTS

<u>Section</u>	<u>Page No.</u>
1. INTRODUCTION	1
2. MODELS AND INSTRUMENTATION	3
3. WIND TUNNEL TESTS	4
4. RESULTS	6
4.1 Flow Visualization	6
4.2 Side Force Data	8
4.3 Hot Wire Data	11
5. CONCLUSIONS	13
6. FUTURE WORK	14
7. ACKNOWLEDGEMENTS	14
REFERENCES	14
FIGURES 1 THROUGH 11	16
LIST OF SYMBOLS	48

1. INTRODUCTION

The effects of asymmetric vortex formation in the wakes of slender missiles and aircraft flying at angles of attack between say 30° and 60° and Mach numbers less than about 1.2 give rise to potentially serious control problems. For vehicles in this pitch range the asymmetric flow patterns produce large forces and moments in the yaw plane. These effects have been investigated by several workers (refs. 1-4). If the induced, out-of-plane effects were constant in direction, the problem of control might not be too severe. However, the forces and moments can change sign, unpredictably, with consequent more serious implications for the possibility of control.

The potential seriousness of the controllability problems has prompted several investigations into means for modifying or alleviating asymmetric vortex effects (refs. 3, 6, 7, and 8). These have made use of specially shaped bodies, disturbance of the flow by ejecting air from the body and strakes or vanes to influence flow development.

The changing sign of the yaw plane forces and moments is held to have a least two possible origins. First, circulation-bearing eddies in the free stream; these may strike the body, causing a change in the net circulation about it, thus producing a different wake configuration (ref. 5). Second, the influence of manufacturing imperfections on the body surface; these are thought to be the basic cause of steady asymmetric wake development. It is hypothesized that they cause the boundary layer to develop asymmetrically on the body, resulting in premature separation on one side before the other, leading ultimately to the formulation of asymmetric wake vortices. The changing disposition of these imperfections relative to the wind vector as the angles of attack or roll are changed produces changing sign and/or varying magnitudes of the out-of-plane forces and

moments. The variations with change in attitude have been the more widely observed in practice. The present work concentrates on the effects of changing roll angles. In what follows the term "roll" will be used to denote static situations where the angle is changed incrementally.

The importance of roll attitude on out-of-plane force and moment signs and magnitudes has been noted by several authors (refs. 1-3). It was found that by changing roll angle the forces and moments could be changed in cyclically repeatable fashion. It was possible to produce the effect by rolling a complete nose-cylinder body, the nose section and the cylindrical section aft of the nose (ref. 3). Even rolling the nosetip alone produced the effect (ref. 1). Since missiles and aircraft may change roll attitude in flight, the consequence for controllability are clear. However, the cyclic, repeatable nature of the changes in out-of-plane forces and moments with roll angle leads directly to the present concept for control. In what follows the terms "rotation" and "spin" will be used to denote dynamic situations where the angle is changed continuously.

It had been observed that if the body is rotated about its axis, the forces and moments vary cyclically with time (ref. 3). This means that the force variations are cyclical and determinate instead of random. In addition, if the rate of variation is high compared with the response time of the vehicle, then it would be expected that the body would behave as though subjected to the time-average of the out-of-plane effects, leaving the vehicle free, on the average, from varying forces and moments. However, spinning the entire body is not usually a feature of vehicle design. On the other hand, it had been found that the nose, nosetip or afterbody could also be rolled incrementally to produce a repeatable effect. The present investigation was undertaken to determine if these pieces could be rotated to

yield cyclical rather than random variations and the time-averaged effect.

A further effect of rotating the body pieces was hoped for; a reduction in magnitude of the out-of-plane quantities. Since the wake vortices are supplied with vorticity from the separating boundary layer, changes in boundary layer development might alter the quantity of vorticity being shed from the body. Any reduction should be reflected in reduced vortex strength and in the related forces and moments. In addition, since the wake pattern was expected to change, the vortices might not have enough time to develop their flow fields fully, before switching to a new pattern. This might also lead to reduced effects. Indeed, Kruse (ref. 4) found during recent tests on a cone spinning up to about 8 rps that the magnitude of the side forces reduced with increasing spin rate.

It was decided, with ultimate hardware application in mind, to test models which featured a spinning nose and nosetip. In addition, since it seems impractical to spin a complete afterbody, a band of the body surface just aft of the nose was spun also.

2. MODELS AND INSTRUMENTATION

The basic model was a 2.6 inch diameter cylinder with a tangent-ogive nose, 2.5 calibers long. Overall length was 15.5 calibers. The model was deliberately made quite slender to permit development of an extensive asymmetric vortex pattern. The body was composed of two major sections. At the upstream end, the first 6.5 calibers contained the spinning devices and their drive mechanisms. Two separate arrangements were used. One permitted test of the spinning nose and nosetip, figure 1a. The other contained the spinning band, figure 1b. Spin was accomplished by means of d.c. motors. Spinning-segment angular

position was recorded by means of a 256 step optical encoder so that out-of-plane quantities could be compared at the same roll positions. Spin rate was monitored by a photoelectric cell. The models were made mainly of steel and aluminum. However, the spinning devices were made of magnesium to reduce possible dynamic effects due to imbalance. Subsequent investigations showed no measurable imbalances during test. The devices could be spun from 2 to 100 Hz in the clockwise and counterclockwise directions. They could also be rolled incrementally, a few degrees at a time, to investigate the detailed behavior during a roll cycle.

Aft of the spinning device section was a cylindrical section 9 calibers long. This contained the six-component balance and, near the rear, three hot wire anemometers mounted flush with the surface. These were distributed around the circumference at an axial position 2 calibers from the base, figure 2. Although the anemometers were not calibrated, their outputs were used to determine the extent to which the surface flow pattern was influenced by the rotating pieces.

Flow patterns were recorded by means of four cameras. One still and one movie camera were positioned downstream of the model, fixed to the support assembly. These were focused upstream and were used in conjunction with the tunnel vapor screen apparatus. One still and one movie camera were located outside the tunnel. These took photographs and film while the tunnel was filled with enough water vapor to produce "vortex trails" under ordinary tunnel lighting.

3. WIND TUNNEL TESTS

The tests were carried out in the 6- by 6-Foot Supersonic Wind Tunnel at NASA/Ames Research Center. The tunnel was run in the subsonic mode, at Mach numbers of 0.25, 0.6, and 0.85. Both

force and moment tests and flow visualization were performed. Moments were referred to the approximate center of model length. Model angle of attack was varied between 30° and 58° . Data from the balance and hot wires were recorded in three ways:

(a) On the Beckman system which passes balance output through a 5 Hz low-pass filter, samples once per second and produces an average of three readings.

(b) On magnetic tape. Analog data were taken and subsequently digitized for analysis.

(c) On visicorder paper strip. This provided an instantaneous record of model behavior and the ability to guide test development.

The testing typically proceeded as follows: first, the model was pitched from 30° to 58° and out-of-plane quantities were monitored every 5° . Angles at which the maximum magnitudes were observed were selected for further study. The model was set at one of these angles and the incremental-stepping capability was used to roll the devices to various angular positions, a few degrees at a time. In this way, the detailed behavior of side force and yawing moment could be observed during a cycle. Because of an instrumentation difficulty with the encoder, the incremental-stepping data were not completely accurate in roll position. Thus, it was not possible to compare the curves of C_Y at zero and non-zero spin rates. However, the zero-spin-rate extrema in forces and moments could be determined for comparison with the spinning variations. Following the incremental-roll tests, the devices were spun at rates from ± 2 to ± 100 Hz (+ spin was defined as clockwise, looking forward).

The devices were spun with their surfaces smooth and then with artificial disturbances fixed to them. This permitted examination of the effect of small disturbances under controlled

conditions. The disturbances took the form of axial strips of grit or tape.

More detail of the 1/2-caliber nosetip grit patterns is shown in figure 3. The various arrangements were: a smooth tip, one axial grit strip, two strips, 180° apart, three equally spaced strips, and a completely gritted tip. The nose was tested smooth and with three tape strips running along its length. The strips were tapered toward the tip. The 1/2-caliber spinning band was tested only with three axial tape strips.

Following the aerodynamic testing, dynamic tests were carried out to determine the resonant frequencies of the complete test set up including model, balance, and support system. By means of a shaker and of artificially-induced imbalances, these natural frequencies were found to occur at about 12, 18, 24, 33, and 42 Hz. The entire system was found to have faithful frequency response up to at least 70 Hz.

4. RESULTS

The most important result of the tests was that the spinning device concept seems to work as expected. The force, moment, and hot wire data, plus the flow visualization work show this clearly.

4.1 Flow Visualization

Flow visualization studies will be discussed first. These showed that the wake vortices could be changed to a large variety of apparently stable patterns by incrementally rolling the nose, nosetip and band. In addition, the patterns could be changed at various frequencies by spinning the devices. The most striking results were obtained with artificial disturbances present (grit and tape strips). However, the smooth nose and nosetip were also effective in changing the flow. Several flow

visualization photographs taken at various random roll positions are shown in figures 4-6. The photographs were taken at $M = 0.6$, which proved to be best suited for flow visualization. All devices shown have artificial disturbances, viz three tape strips on the nose and band; three grit strips on the noisetip. Figures 4a, b, and c show the effect of the band, using the vapor trail technique. The same technique was used for figures 5a, b, and c which show the effect of the noisetip. Figures 6a, b, c, and d show the same configuration as figure 5 (photographs not correlated) using the vapor screen technique. It is clear that considerable changes in the wake patterns can be produced by the band and the noisetip. The effects of the nose and nose-tip are shown in a movie, taken at $M = 0.6$ and $\alpha \sim 50^\circ$.

The movies showed that the vortex pattern switching was approximately synchronized with the device rotation rate and the number of disturbances. In the cases of the nose and noisetip, the entire wake switched from the tip of the nose to the base. With the band, the two vortices generated on the nose upstream of the band remained unchanged, but the rest of the pattern varied with spin rate. At low rotation rates the individual vortices retained their definition and their motion could be followed visually. At high rotation rates, the pattern varied so fast that it became impossible to identify individual vortices. However, at these speeds the evidence of the balance and hot wires showed that the pattern continued to change with spin rate (see later). The response was probably related to the time required for disturbances to traverse the length of the body. At the lowest Mach number (0.25) the time required for a fluid particle to traverse the length of the body was about 1/50th of a second at $\alpha = 50^\circ$. With a maximum rotation rate of 100 Hz, disturbances produced near the nose would be transmitted downstream at a maximum rate approximately equal to $1/100p$, where p is the number of disturbance-causing mechanisms

(artificial or natural) per cycle. Hence, during the $M = 0.25$ tests disturbances were introduced at frequencies higher than required to ensure that more than one disturbance was influencing the pattern at a given time. At the higher Mach numbers (0.6, 0.85) fewer conditions existed where more than one disturbance was present in the flow pattern at a given instant.

4.2 Side Force Data

Turning now to the results from the six-component balance, attention will be focused on side forces. Yawing moment behavior was essentially the same as for side force. Some limited discussion of pitch plane quantities will be given later. Axial force and rolling moment were not expected to vary significantly and are not discussed.

The analog tape data were first digitized and then treated by linear ensemble averaging. This process essentially involves averaging by super-position of individual data cycles, one on top of the other. If a coherent signal is contained in the data, but its form within a given cycle is masked by random noise, the process averages out the noise, leaving the signal. It was found in most cases that after superposing as few as five cycles the signal emerged. After twenty to thirty cycles were averaged the signal was found to be unchanged. Eventually fifty cycles were averaged, to ensure that the noise had been completely removed. Examples of ensemble-averaged side force coefficient are shown in figure 7.

The repeatability of the data is clear, corroborating the evidence of the flow visualization studies. Cyclical switching of the vortex patterns is taking place, repeatably, resulting in cyclical force variations. Another hoped-for effect, that of reduction in side force variation, may be seen by comparing the peak-to-peak variation in C_y across the speed range, with the static or incrementally-rolled C_y variation ($n = 0$). The results

are shown in figure 8 for the nose and nosetip. No zero-spin data are available for the band. However, the spinning band data do show very small C_Y variations. The fully-gritted nosetip and the smooth nose had only small effects and are not shown. It may be seen that in most cases side force variation is reduced even at spin rates below the lowest resonance frequency of 12 Hz. From the known-imbalance tests, comparisons between applied centrifugal force and balance reading indicated that dynamic effects could cause uncertainties in the values of C_Y read from the balance. These effects were estimated to be about $\pm 50\%$ of the balance reading. Uncertainty bands are shown on the data in figure 8 for spin rates of 10 rps and above. Also shown in figure 8 is the mean of the data found by Kruse (ref. 4) for a spinning cone. It will be seen that in most cases the trends and magnitudes of the two sets of data are quite similar.

Figure 7 shows the effects on C_Y of the various devices, their spin rates and directions. Note that in figure 7, whether spin is positive or negative, the abscissa always gives ϕ from 0 to 360° in the direction of spin, i.e., both positive and negative roll angles run from left to right. Figure 7a and b show the effects of the tip with a single grit strip at 20 rps. It will be seen that the force magnitudes are greater with positive spin. This may be due to the presence of other, natural disturbances on the body. However, the variations in the curve shape imply that when the grit strip was at a given angular location, the flow pattern was essentially the same, whether the strip arrived there from the positive or the negative direction. On the other hand, figures 7c and d show that the tip with two axial grit strips seems to generate a flow pattern repeatable each 180° but with an apparent phase shift of 90°. This is believed to be due to a damaged connection which allowed backlash in the drive mechanism to the encoder. The three-strip data were quite unlike for different spin directions. In addition, varying the spin rate changed the characteristics of the side force curves, as shown in

figures 7e, f, g, and h, implying a distortion of the flow pattern. This result is different from that of reference 4 in which the side force curve shapes remained similar with changing spin rate. Figures 7j-7l show the nose with three tape strips at various speeds. It will be seen that here too the curves show distortion as speed is increased. The question of possible wake distortions is discussed later, in connection with the hot wire data. Finally, a typical curve showing the effect of spinning the surface band with three tape strips is shown in figure 7m. It will be seen that the variations are much smaller than for the nose and tip. This may be due to the condition of the boundary layer at the band. The layer will be much thicker and more resistant to surface disturbances than that near the nose. On the other hand, the flow studies showed that the band changed only the wake aft of itself, leaving unchanged the two vortices on the nose. It may be that these vortices play a dominant role in side force variations. When they remain unchanged, this seems to reduce the force variation on the body over a cycle.

The cyclic side forces do not average out to zero in all cases. However, their rates of change are so rapid that when applied to a body with low natural frequency of aerodynamic response (missiles typically have natural pitch and yaw frequencies of 3-5 Hz) the effect should be an averaging of the impulses by the system. This conclusion is supported by the Beckman system data shown in figure 9. Here, the range between maximum and minimum C_Y over a cycle at zero spin rate is compared with the filtered, averaged data at spin rates up to ± 100 rps. The zero spin rate data indicate the range within which the side force on a body might lie during non-spinning operation. The data points indicate the level of side force which would be experienced by a vehicle having about a 5 Hz natural frequency in yaw. The considerable reductions in side-force variation, even with quite low spin rates, is evident. It appears that the averages usually have values near the center of the zero-spin C_Y range. The single

exception is the data with a smooth nosetip at $\alpha = 55^\circ$. The effect of spin here is mainly to focus the average values of C_y near the upper and lower ends of the C_y range, depending on spin direction. However, not all the points are focused in the same direction by a given spin direction, figure 9d. Because of the 5 Hz filter, some question arises of the validity of the filtered, averaged values in cases where (spin rate \times number of disturbances) is less than 5 Hz. However, this does not apply to the bulk of the data. It should be noted that the averages obtained using the Beckman system did not always correspond to those from the magnetic tape. This discrepancy has not yet been resolved. However the main conclusions on cyclic repeatability, side force reduction and averaging should not be significantly altered because of this.

The results of figures 8 and 9 have important implications for the use of the spinning device concept in practical cases. It appears that a missile employing a spinning device and flying at high angle of attack would probably experience a side force, essentially constant in magnitude and direction. It would also experience some vibration whose severity would decrease with increasing spin rate.

4.3 Hot Wire Data

Changes in the overall flow field will be reflected by changes in the vortex pattern and in the flow on the body surface. The three hot wires placed near the rear of the body showed clearly the effect of spinning the various devices. All three wires showed similar behavior, hence, attention will be focused on only one for the present discussion. Figure 10 shows the response of hot wire #2, which was placed at what would have been the wind-side stagnation point in symmetrical flow. The data are plotted versus encoder position in degrees. Again, 50 cycles of data were ensemble-averaged to obtain the signal (which was not calibrated and hence is presented with no vertical scale). The data show the effect of the nose with three tape strips,

spinning at different speeds. The cyclic repeatability of the signal is clear from the distinct curves obtained. This is consistent with the cyclic repeatability shown by the balance data.

It will be seen that the form of the hot wire curve changes with increasing spin rate. In general, the number of positive and negative peaks in the signal decreases as spin rate increases. However, the decrease in number of peaks is not so rapid or pronounced in the hot wire data as in the balance data (figs. 7j, k, and l). Between 10 and 20 rps, the hot wire shows only a small reduction in number of peaks. At the same time, the balance data show the number of peaks to be about halved. At 50 rps the number of peaks in the hot wire output is further reduced and the signal appears to have a one-per-cycle dominant frequency. The corresponding balance output, figure 7l, shows no discernible pattern. The differing behavior of the hot wire and the balance implies that the flow pattern on the body changes more rapidly than that in the wake. At the highest rate of (spin \times number of disturbances) shown (150 Hz) the balance response may have been dynamically distorted. However, at the lower spin rates this should not have been the case. A possible explanation for the slower rate of wake response may be that the vortices cannot change position quickly or extensively enough at the higher speeds to produce the full side force effect in each cycle. The precise mechanism underlying the phenomena requires further investigation.

This report has concentrated on side forces but a brief mention of pitch angle quantities is in order. Normal force and pitching moment proved to be influenced by the vortex switching, particularly when artificial disturbances were present. Although no reduction was found in their average values, the cyclic variations at zero spin rate could be as much as ± 20 -percent in the case of pitching moment, figure 11. This shows the range of C_M as the nosetip with three grit strips was first rolled

incrementally and then spun up to ± 100 rps. The Beckman data (which again are seen to be close to the average of the cyclic data) show the spread to be collapsed into a very small range. This is an additional advantage of the spinning device concept.

5. CONCLUSIONS

The spinning device concept of actively controlling asymmetric vortex effects appears to work quite well for the cases investigated. Side force variation is drastically reduced with increasing spin rate and the average side force can, in some cases, be brought near zero. In addition, pitching moment variations can be averaged out.

It appears that the flow pattern on the body can be changed more rapidly than can that in the wake. This implies a limit on the speed with which the vortices can change position fully.

The spinning-segment concept has several attractive features relative to other means of influencing yaw forces and moments:

- (a) it should work regardless of the direction in which the body is pitched or yawed
- (b) it requires no carriage of ejectable fluid
- (c) it requires no breaks or steps in the body shape
- (d) it is probably not configuration-dependent and can be universally applied (although this has yet to be fully investigated)
- (e) it requires no additional vanes or strakes
- (f) it appears to have little average effect on pitch plane aerodynamics.

6. FUTURE WORK

The spinning device concept has been shown to work successfully for a long, sharp-nosed, isolated body. It should be investigated for a variety of body lengths as well as for bodies with control fins. In addition, the effect of nose bluntness should be considered. This parameter has been shown to produce marked effects on side force and yawing moment development. It may be that some combinations of nose bluntness, spin rate, and body length will be optimum for a variety of practical applications.

7. ACKNOWLEDGEMENTS

The author wishes to thank NASA/Ames Research Center for the use of the 6-Foot Wind Tunnel, Dr. Gary T. Chapman and Mr. Gerald N. Malcolm, for valuable consultations and suggestions. Thanks are also due to Dr. Jack N. Nielsen for his helpful suggestions. The assistance of the Experimental Investigations Branch at Ames is also acknowledged.

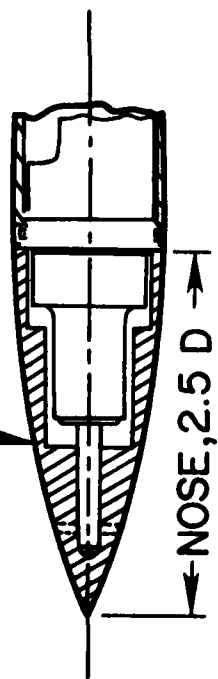
REFERENCES

1. Chapman, G. T., Keener, E. R., and Malcolm, G. N.: Asymmetric Aerodynamic Forces on Aircraft Forebodies at High Angles of Attack - Some Design Guides. AGARD Flight Mechanics Panel, Specialists Meeting "Stall/Spin Problems of Military Aircraft", Paper #16, Nov. 1976.
2. Thompson, K. D. and Morrison, D. F.: The Spacing, Positions, and Strength of Vortices in the Wake of Slender, Cylindrical Bodies at Large Incidences. J. Fluid Mech., 50, Part 4, 1971.
3. Briggs, M. M., Clark, W. H., and Peoples, J. R.: Occurrence and Inhibition of Large Yawing Moments During High Incidence Flight of Slender Missile Configurations. AIAA Paper 72-968, 1972.

REFERENCES (Concluded)

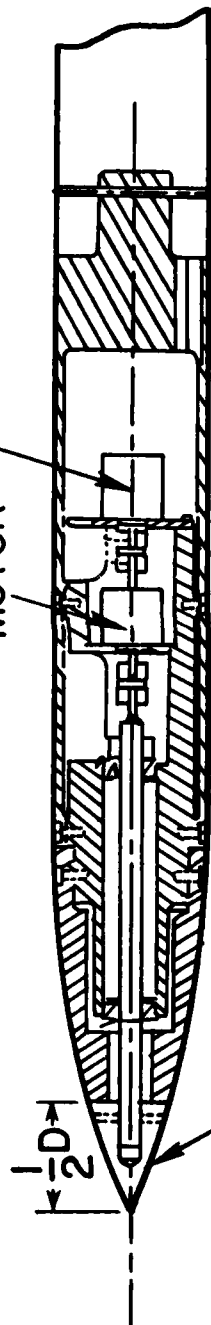
4. Kruse, R. L.: Influence of Spin Rate on Side Force of an Asymmetric Body. J. Space & Rockets, April 1978.
5. Lamont, P. J. and Hunt, B. L.: Pressure & Force Distributions on a Sharp-Nosed Circular Cylinder at Large Angles of Inclination to a Uniform Subsonic Stream. J. Fluid Mech., 76, Part 3, Aug. 1976.
6. Daniels, P.: Ogive Cylinder Modified for Near-Minimum Side Moment. NSWC/DL TR-3873.
7. Sharir, D., Portnoy, H., et al.: A Study of the Effects of Jets Injected from a Slender Body of Revolution on the Side Forces Acting on it at Large Angles of Attack and Low Speeds. Technion, Israel Inst. of Tech., TAE Report 337, May 1978.
8. Titiriga, A., Jr., Skow, A. M., and Moore, W. A.: Forebody/Wing Vortex Interactions and Their Influence on Departure and Spin Resistance. Paper No. 6, AGARD Fluid Dynamics Panel Symposium, Sandefjord, Norway, Oct. 1978.

NOSE (MAGNESIUM)



ENCODER

MOTOR



TIP (MAGNESIUM)

Figure 1a. Models.

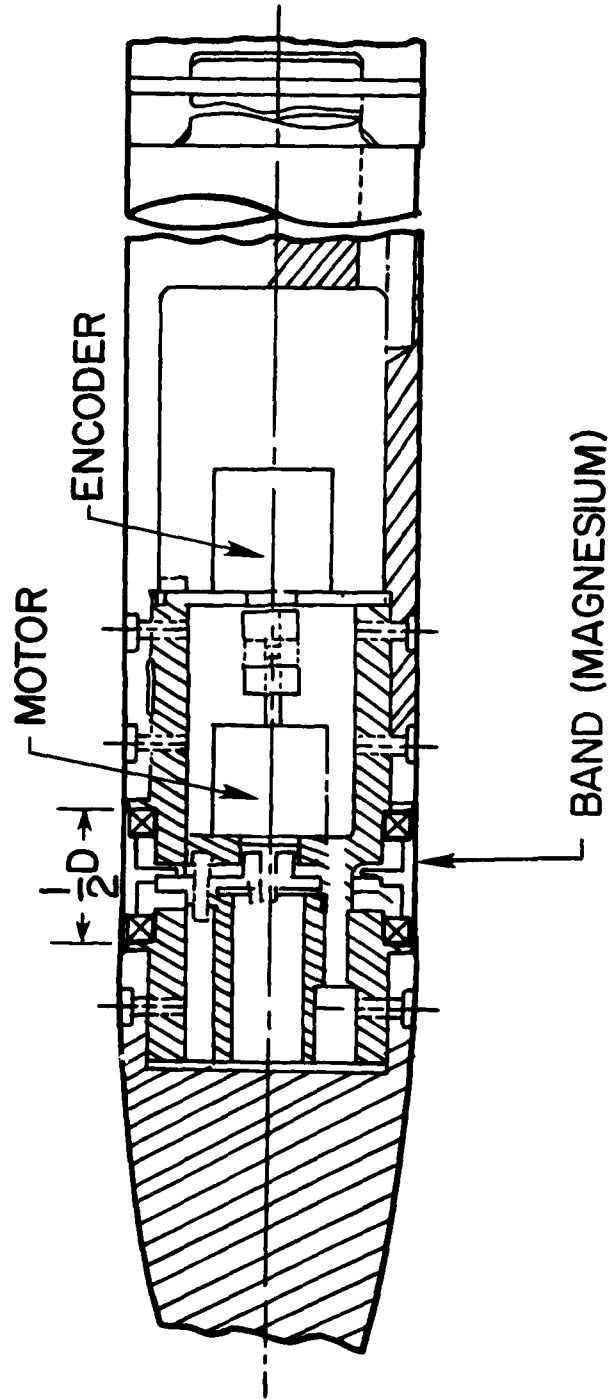


Figure 1b. Models.

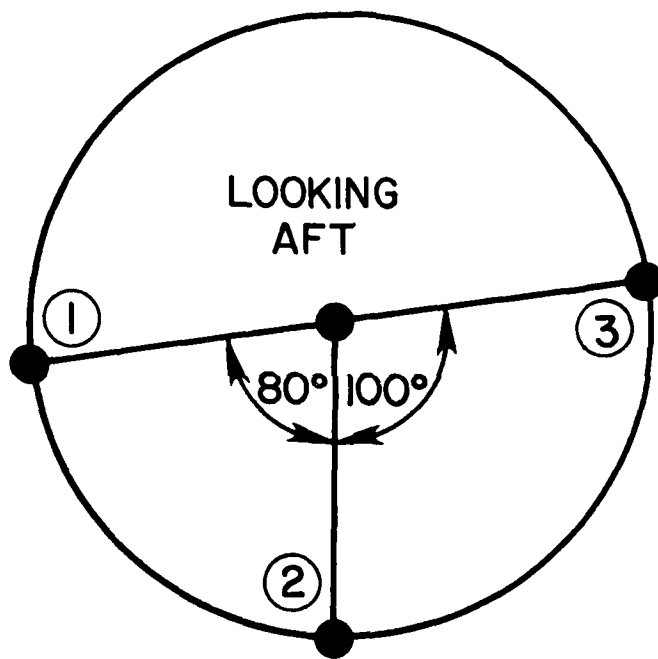


Figure 2. Location of hot wire anemometers around circumference.

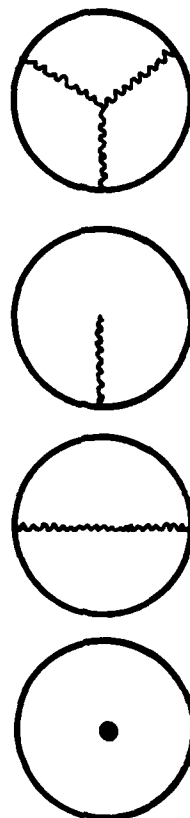
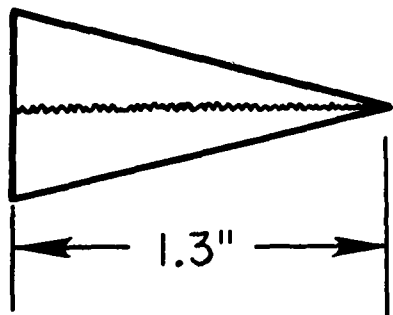


Figure 3. Tip grit patterns tested.



c

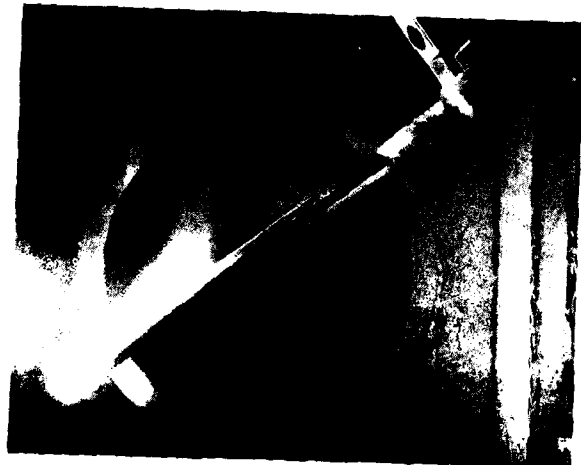


b



a

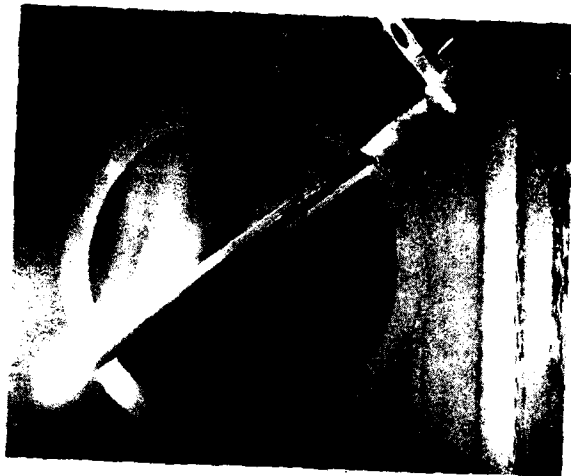
Figure 4.- Effect of surface band on wake vortex pattern at various roll positions, $\alpha = 50^\circ$.



a



b



c

Figure 5.- Effect of noisetip on wake vortex pattern
at various roll positions, $\alpha = 52^\circ$.

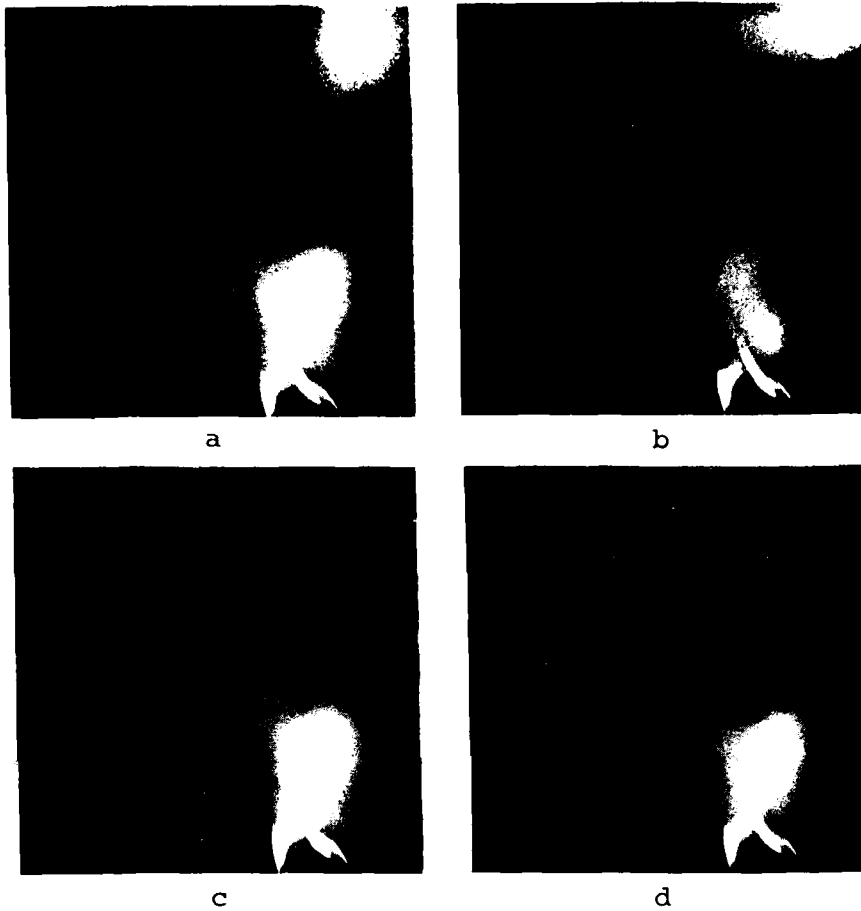


Figure 6.- Effect of nosetip on wake vortex pattern at various roll positions, $\alpha = 52^\circ$.

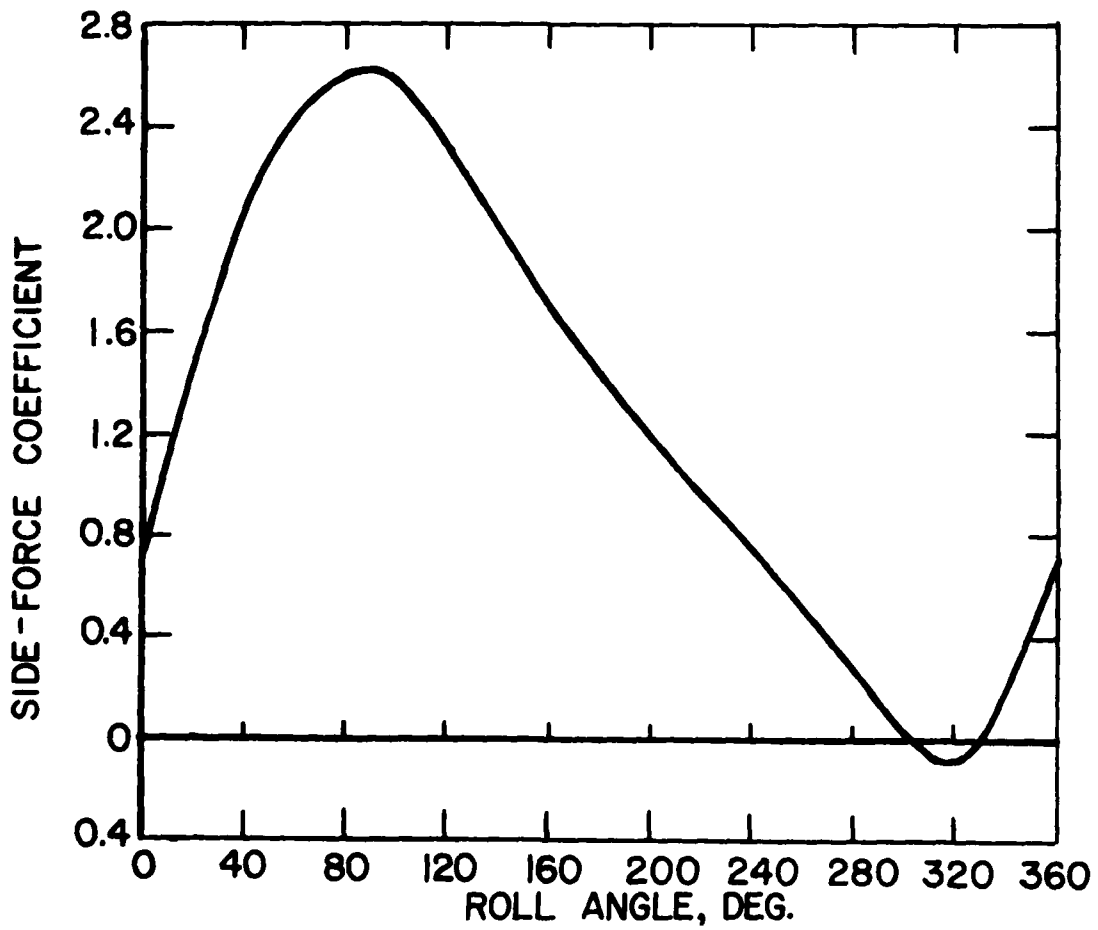


Figure 7a. Tip with 1 grit strip, +20 rps,
 $M = 0.25$, $\alpha = 45^\circ$.

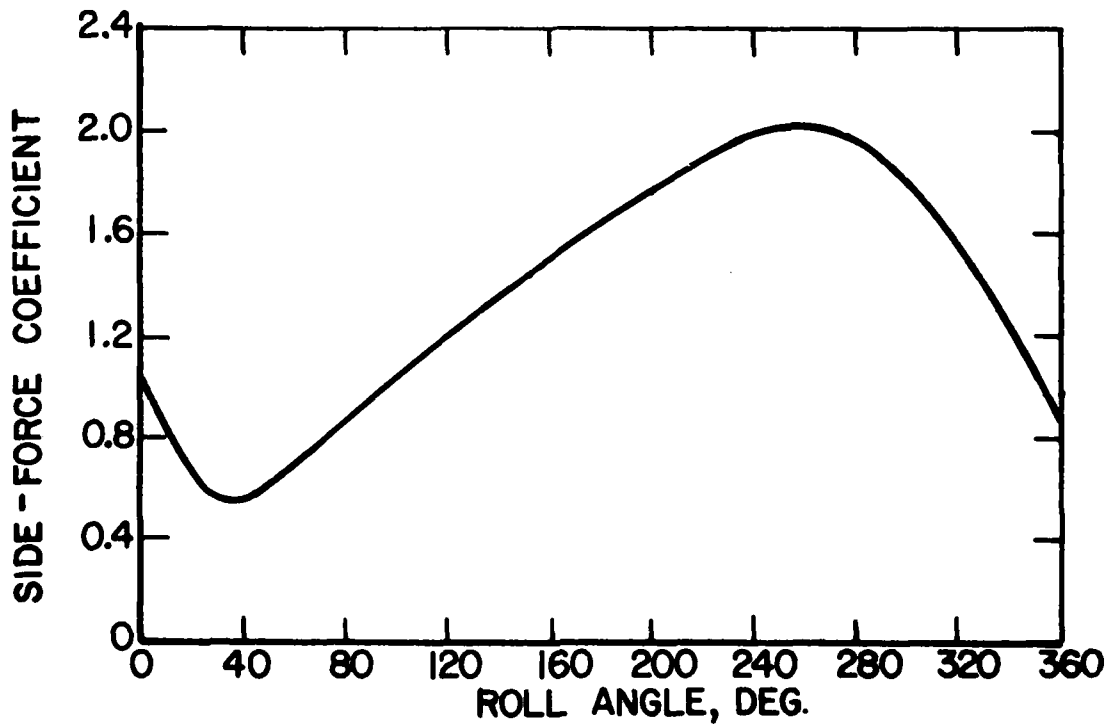


Figure 7b. Tip with 1 grit strip, -20 rps,
 $M = 0.25$, $\alpha = 45^\circ$

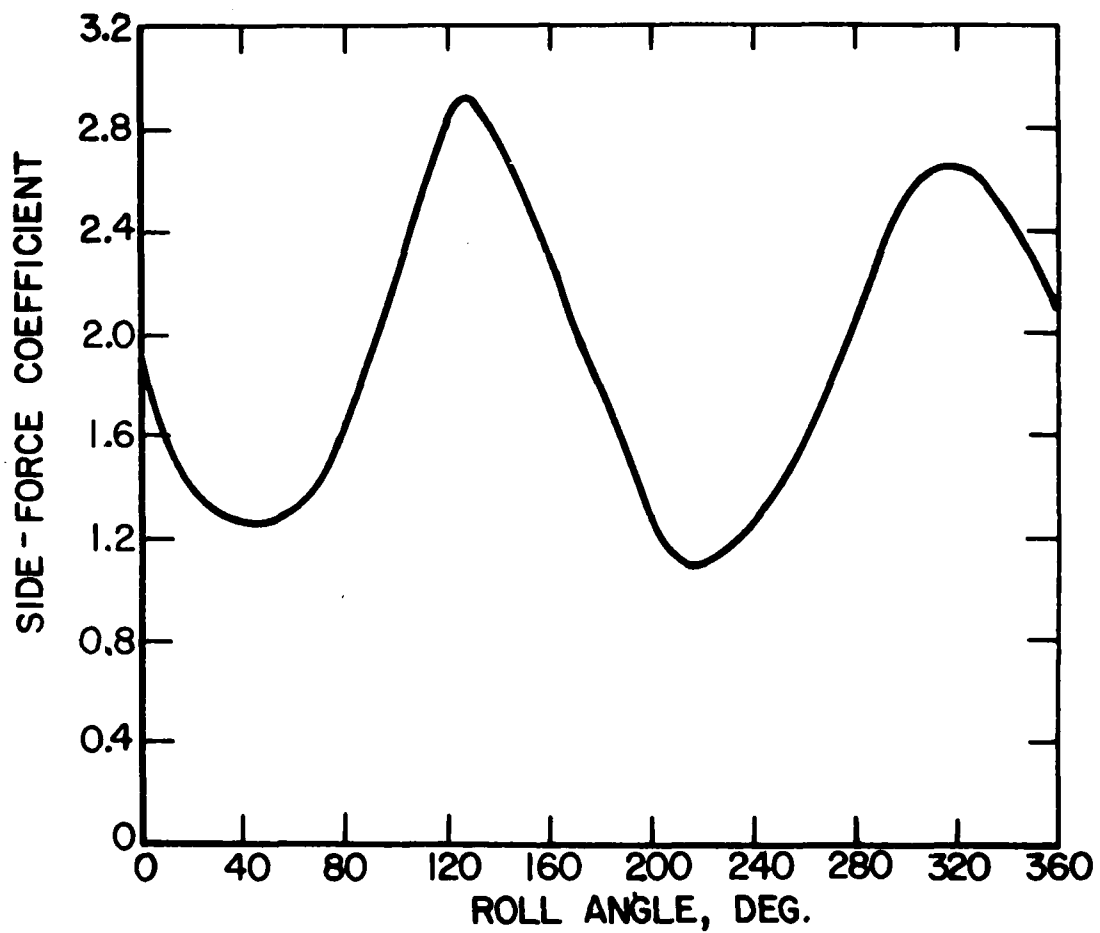


Figure 7c. Tip with 2 grit strips, -10 rps,
 $M = 0.25$, $\alpha = 50^\circ$

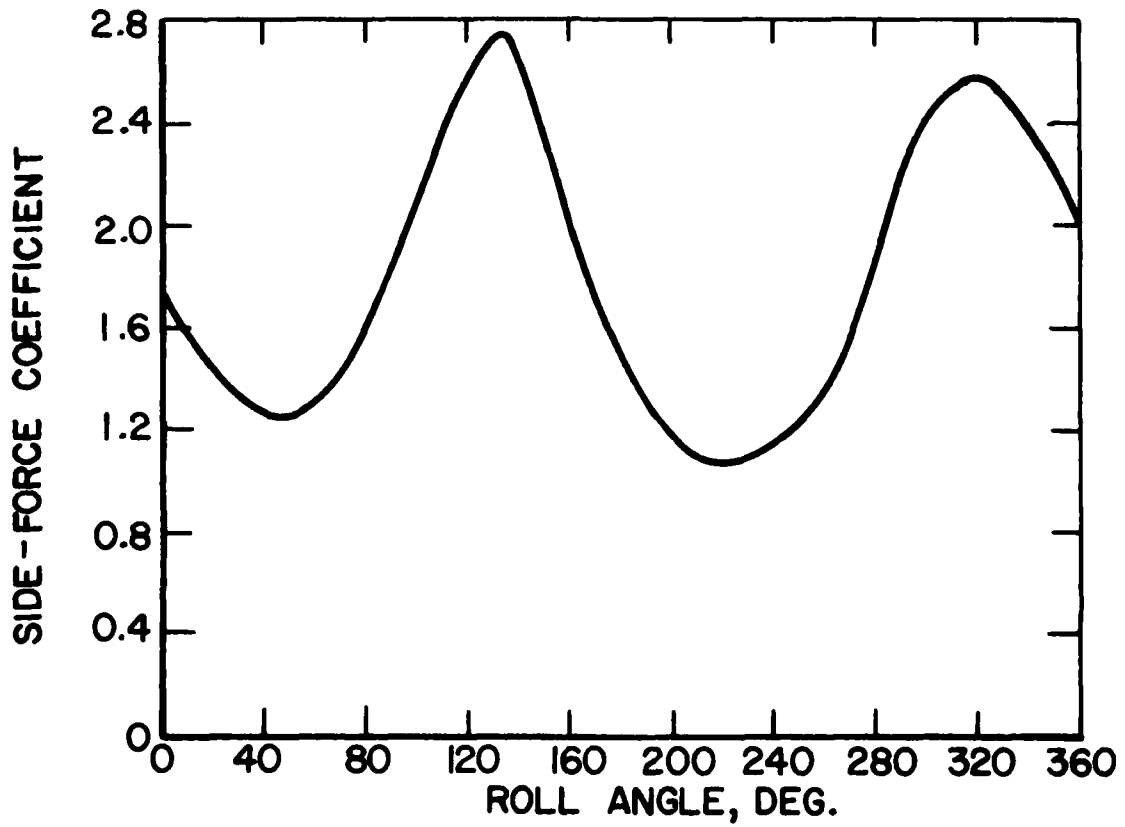


Figure 7d. Tip with 2 grit strips, +10 rps,
 $M = 0.25$, $\alpha = 50^\circ$

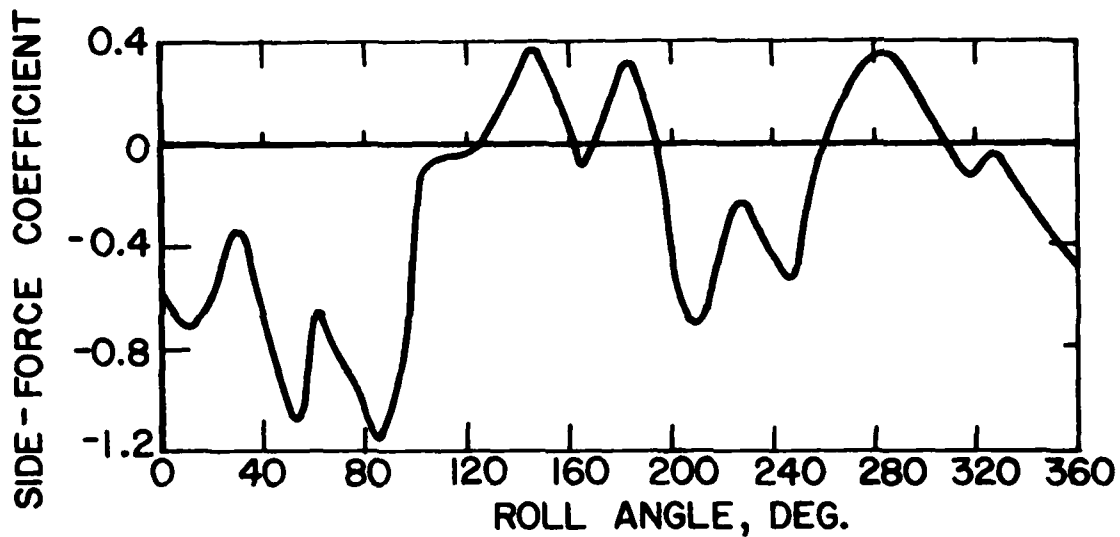


Figure 7e. Tip with 3 grit strips, +2 rps,
 $M = 0.6, \alpha = 30^\circ$

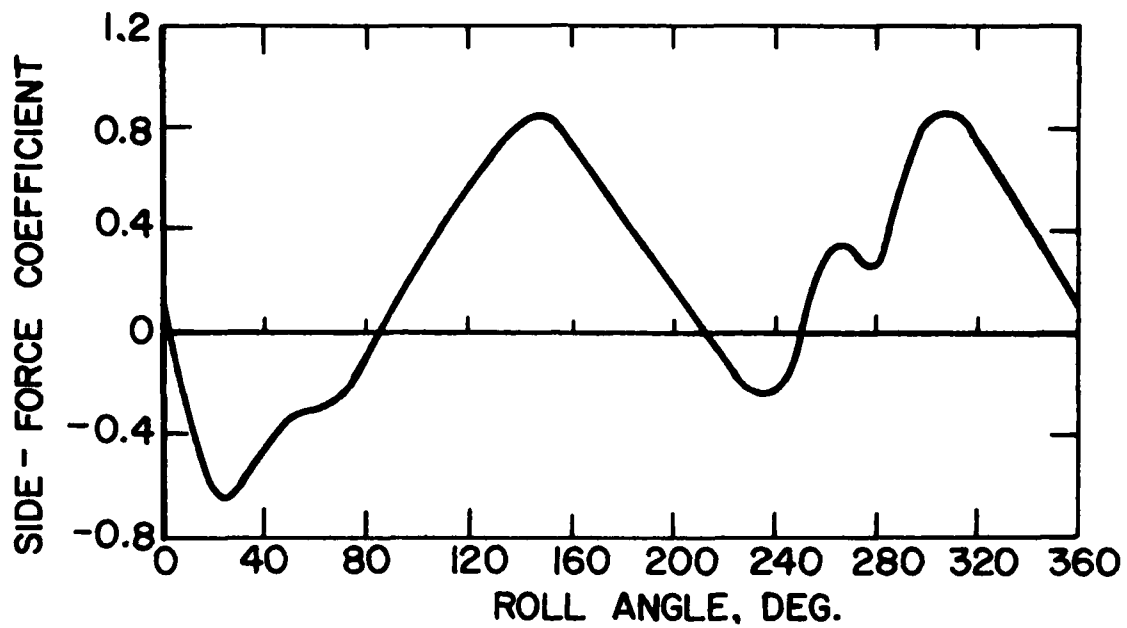


Figure 7f. Tip with 3 grit strips, +5 rps,
 $M = 0.6$, $\alpha = 30^\circ$

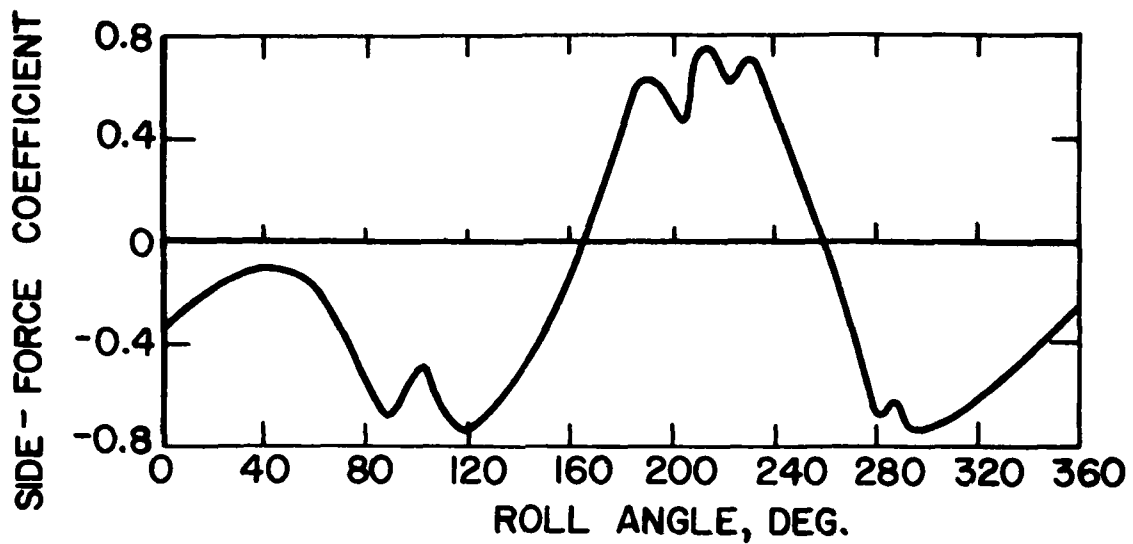


Figure 7g. Tip with 3 grit strips, +10 rps,
 $M = 0.6$, $\alpha = 30^\circ$

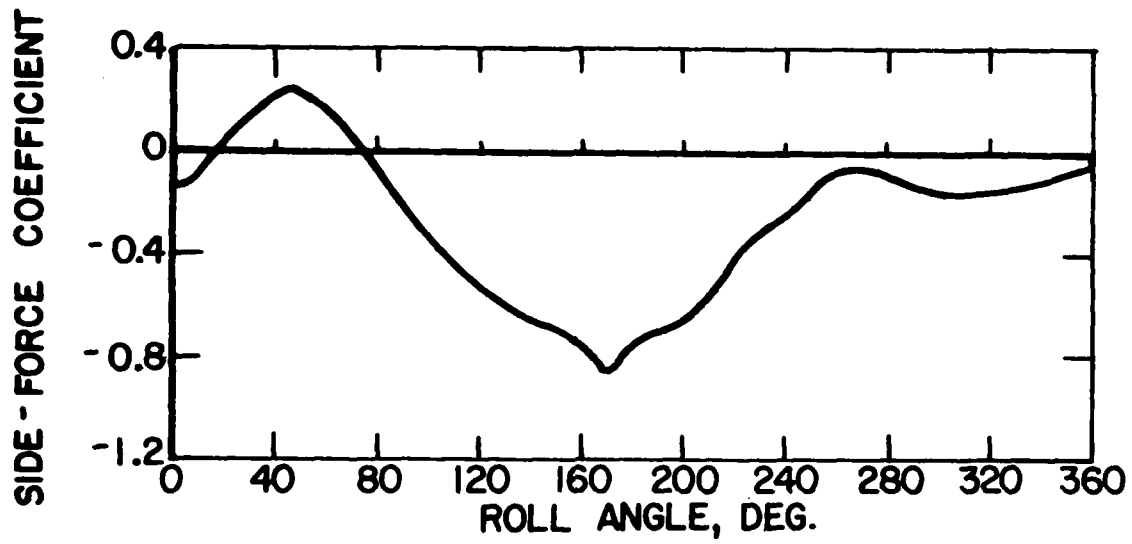


Figure 7h. Tip with 3 grit strips, +20 rps,
 $M = 0.6$, $\alpha = 30^\circ$

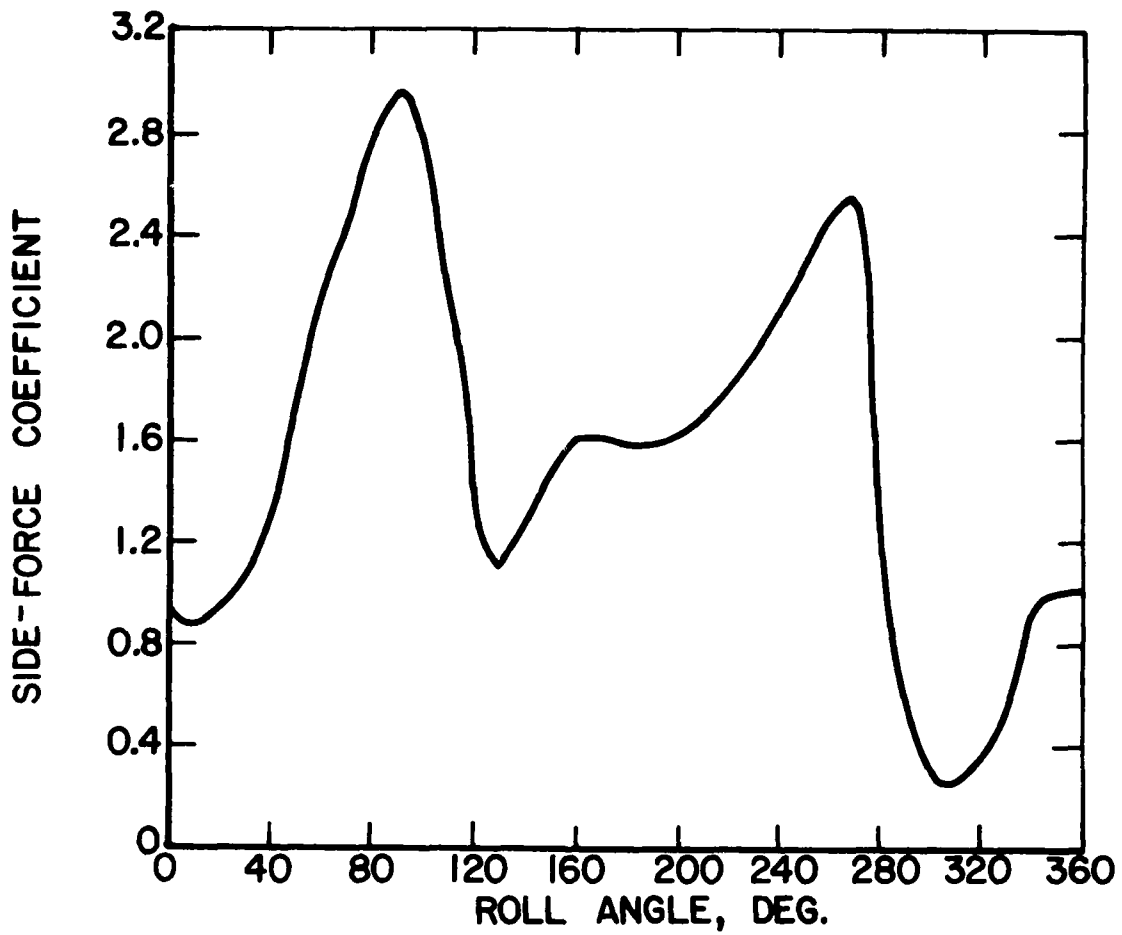


Figure 7j. Nose with 3 tape strips, +10 rps,
 $M = 0.25$, $\alpha = 50^\circ$

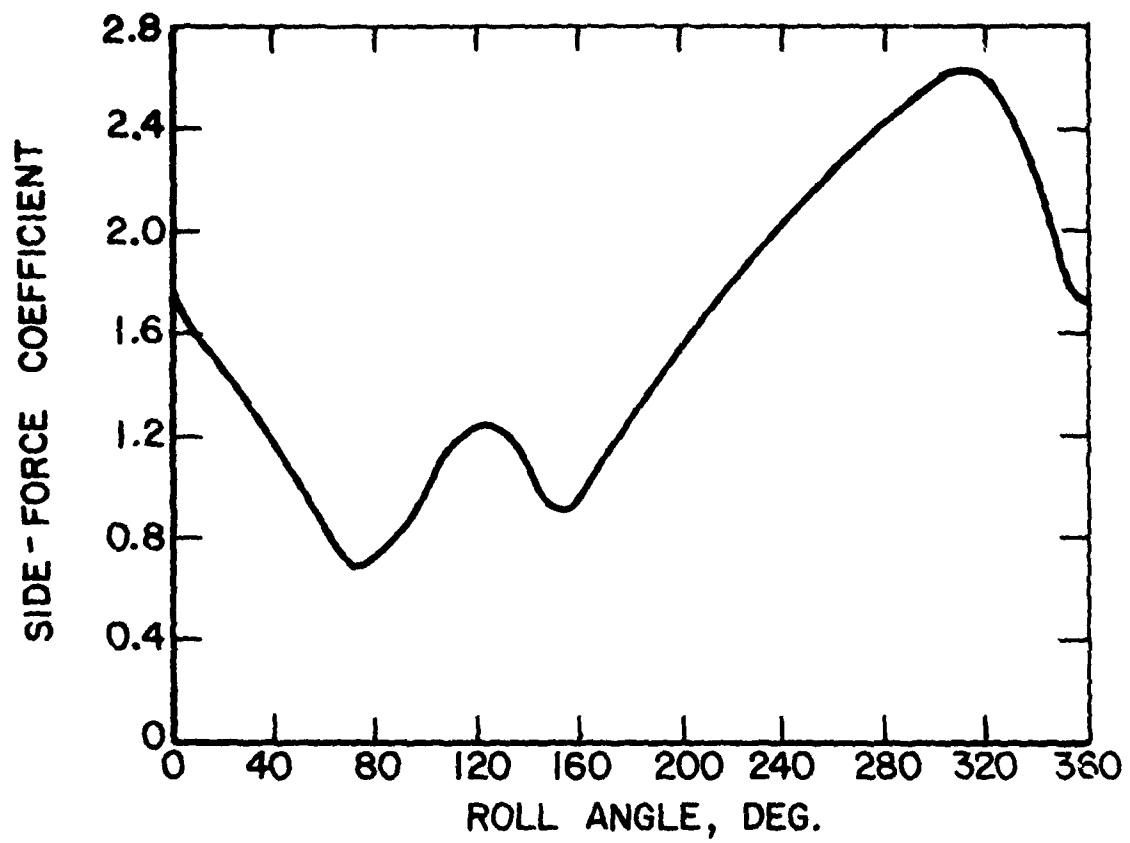


Figure 7k. Nose with 3 tape strips, +20 rps,
 $M = 0.25$, $\alpha = 50^\circ$.

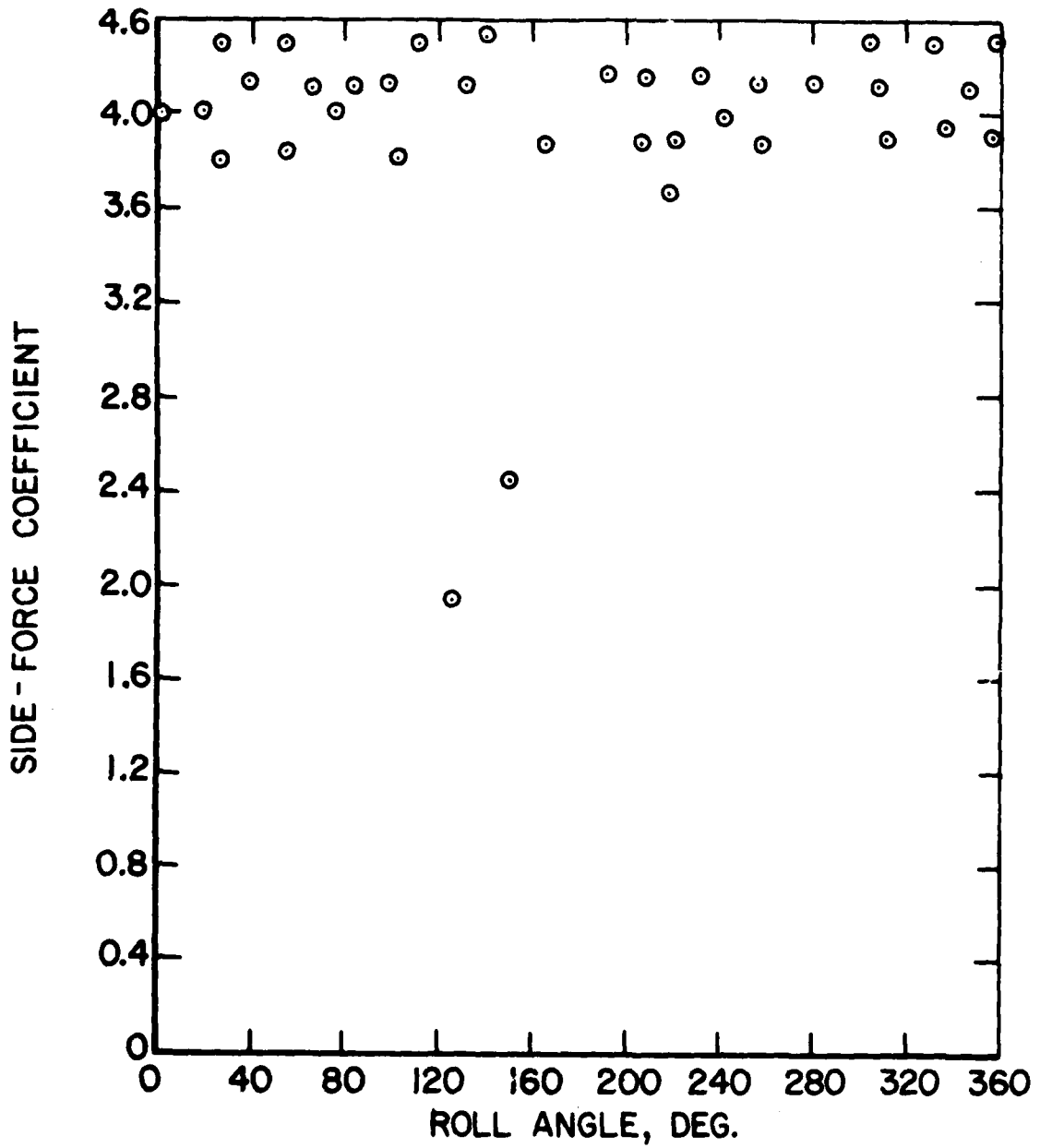


Figure 7*l*. Nose with 3 tape strips, +50 rps,
 $M = 0.25$, $\alpha = 50^\circ$

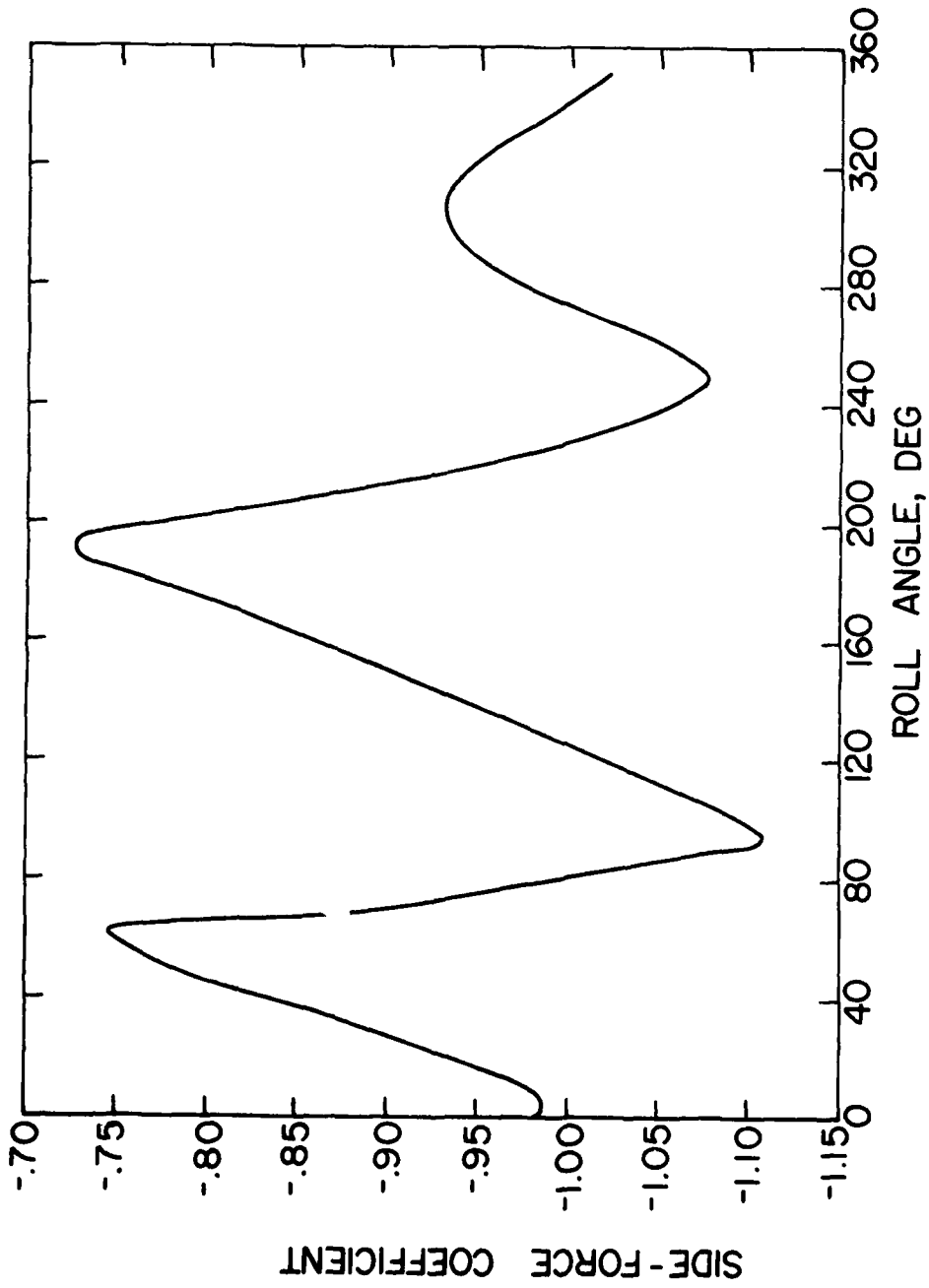
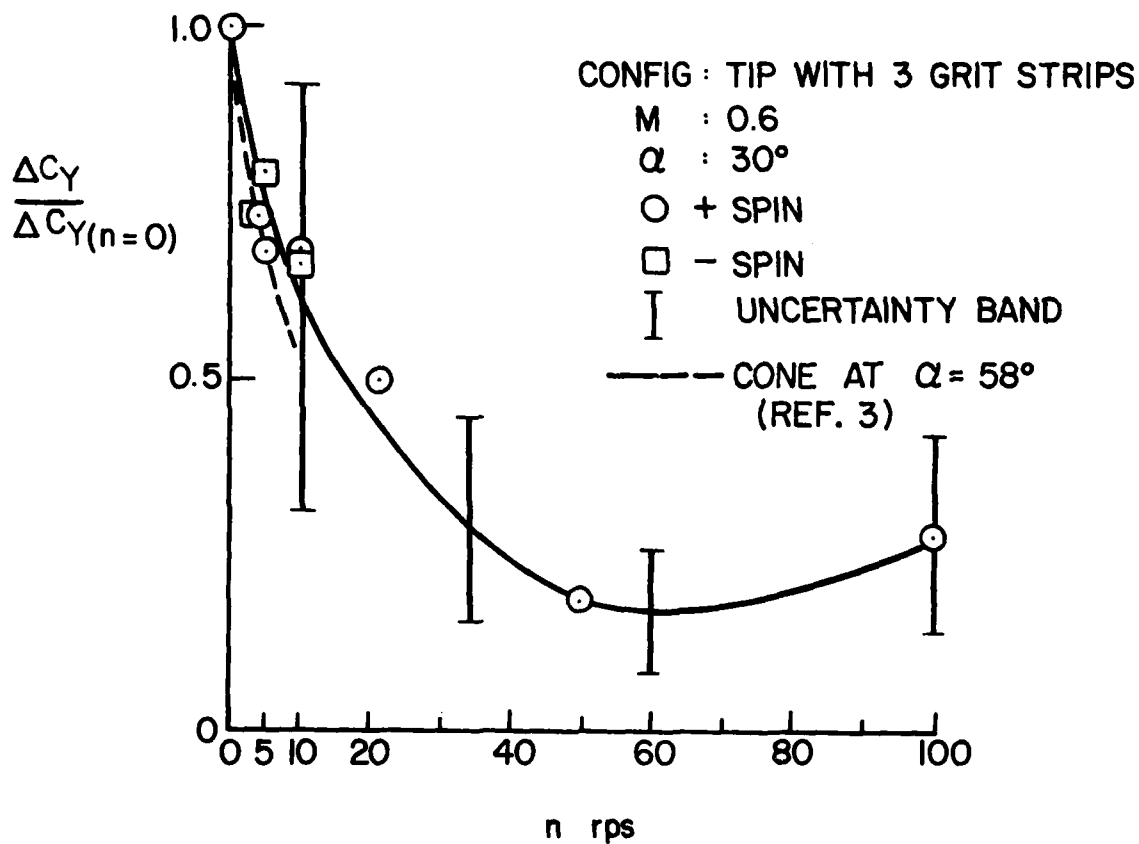
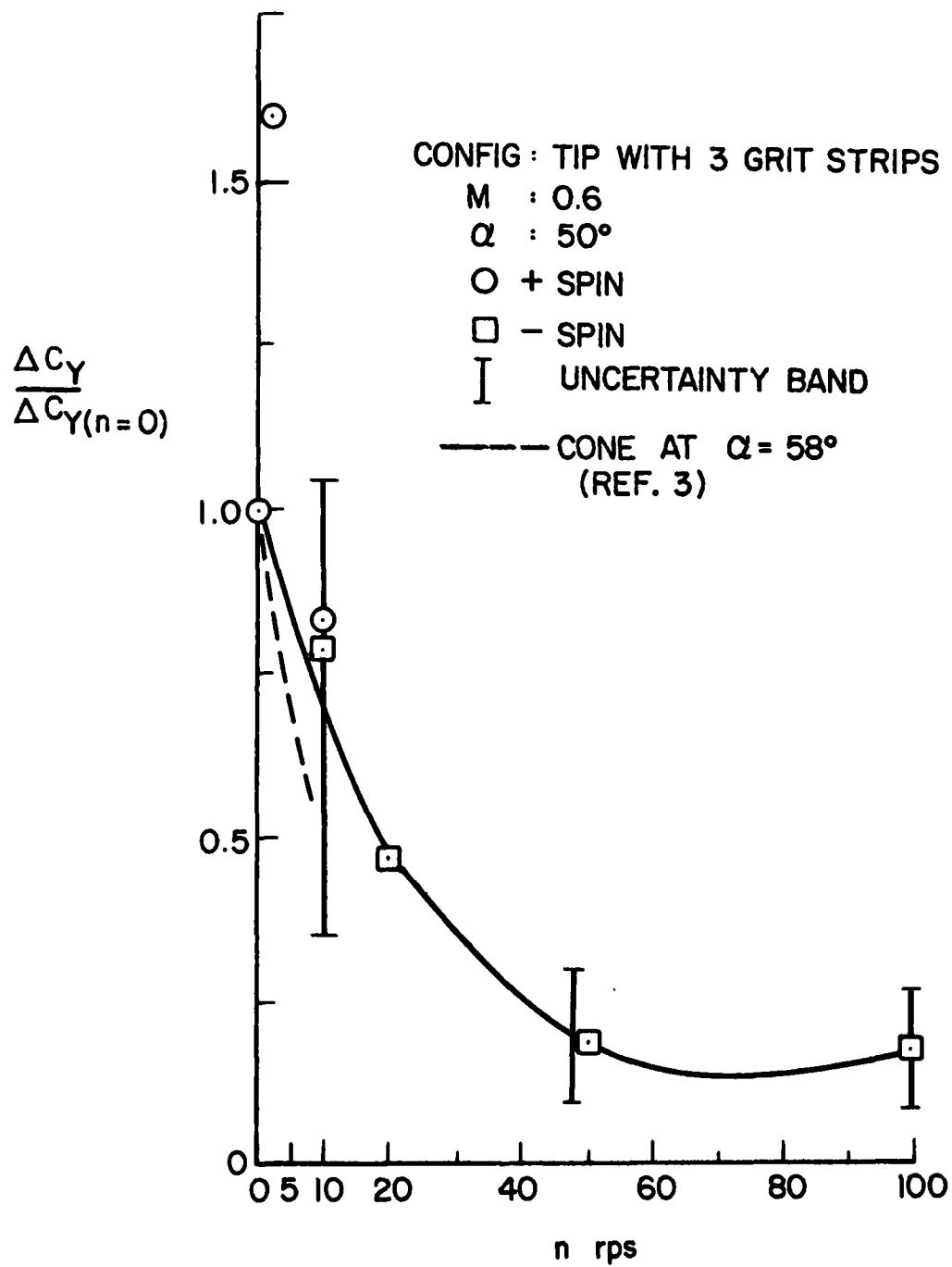


Figure 7m. Band with 3 tape strips, -10 rps,
 $M = 0.25$, $\alpha = 40^\circ$



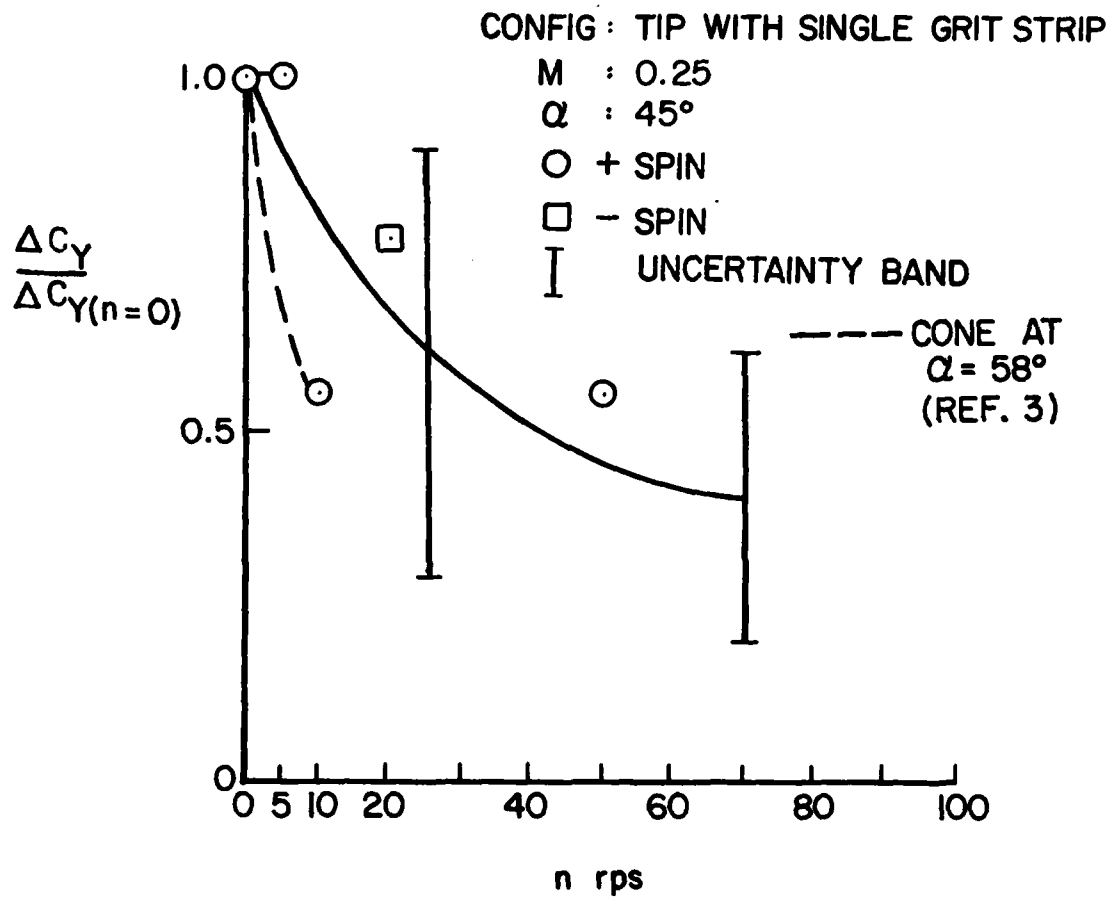
(a)

Figure 8. Side force cyclical variation as a function of spin rate.



(b)

Figure 8. Continued.



(c)

Figure 8. Continued.

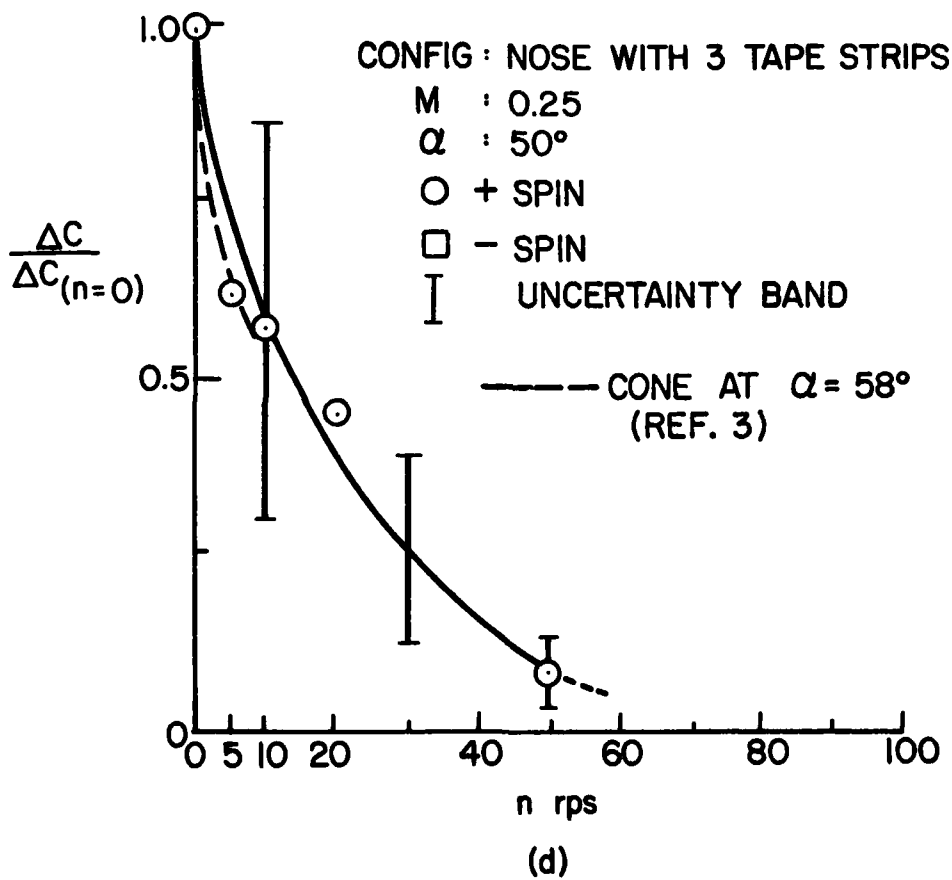


Figure 8. Continued.

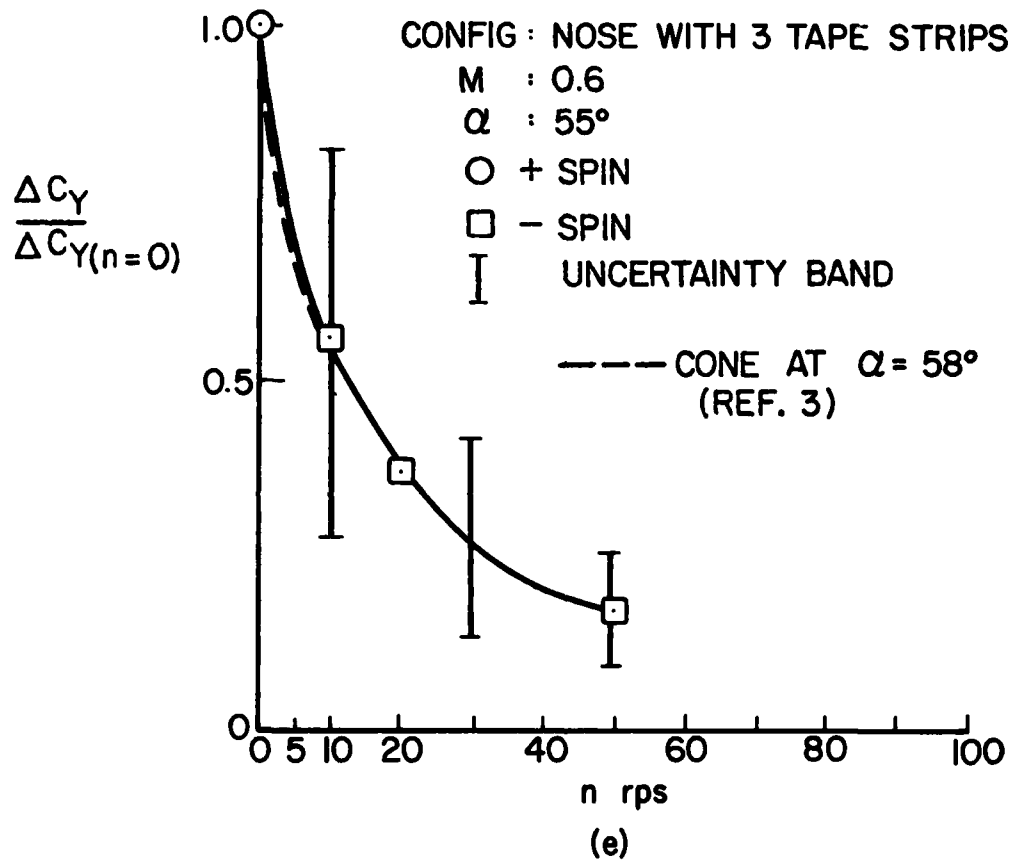
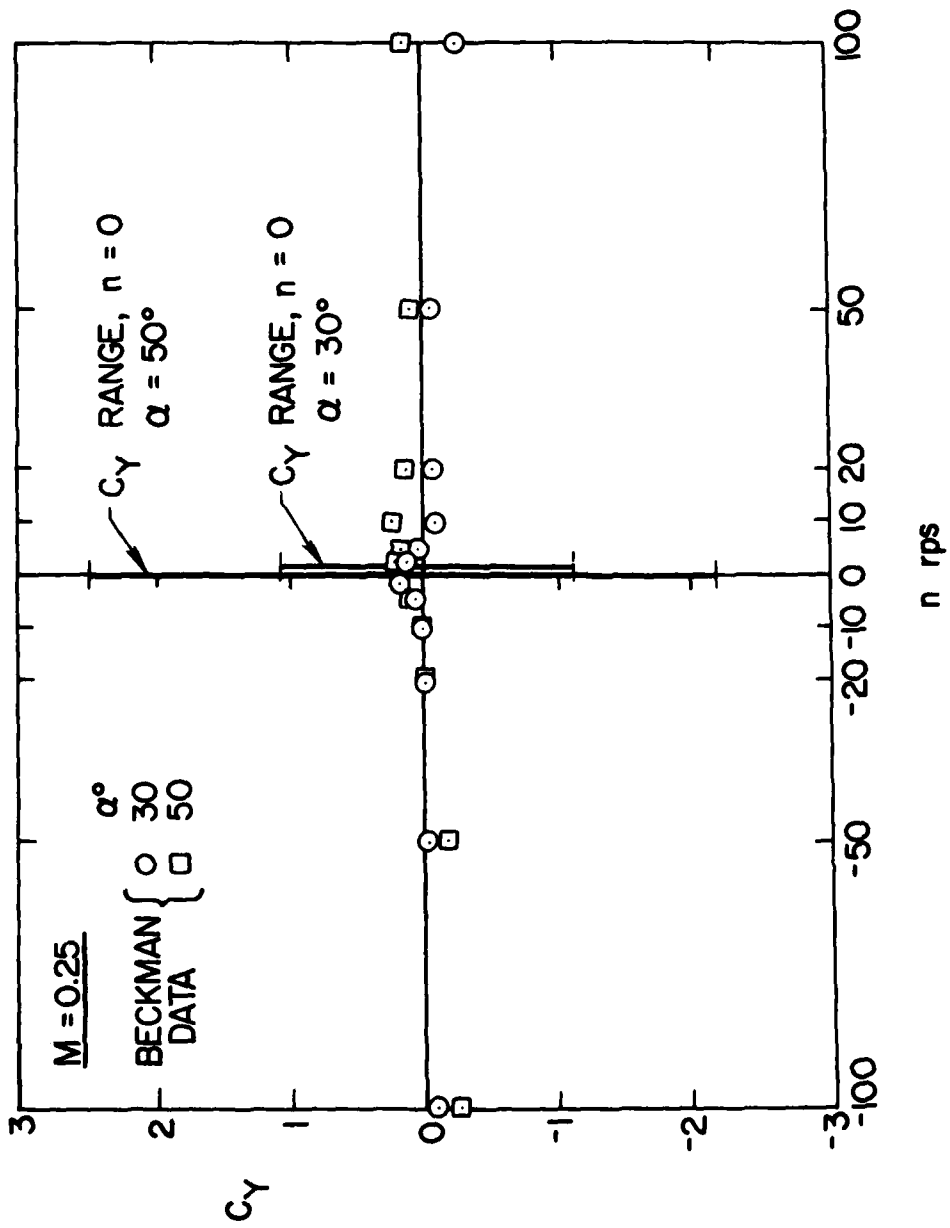
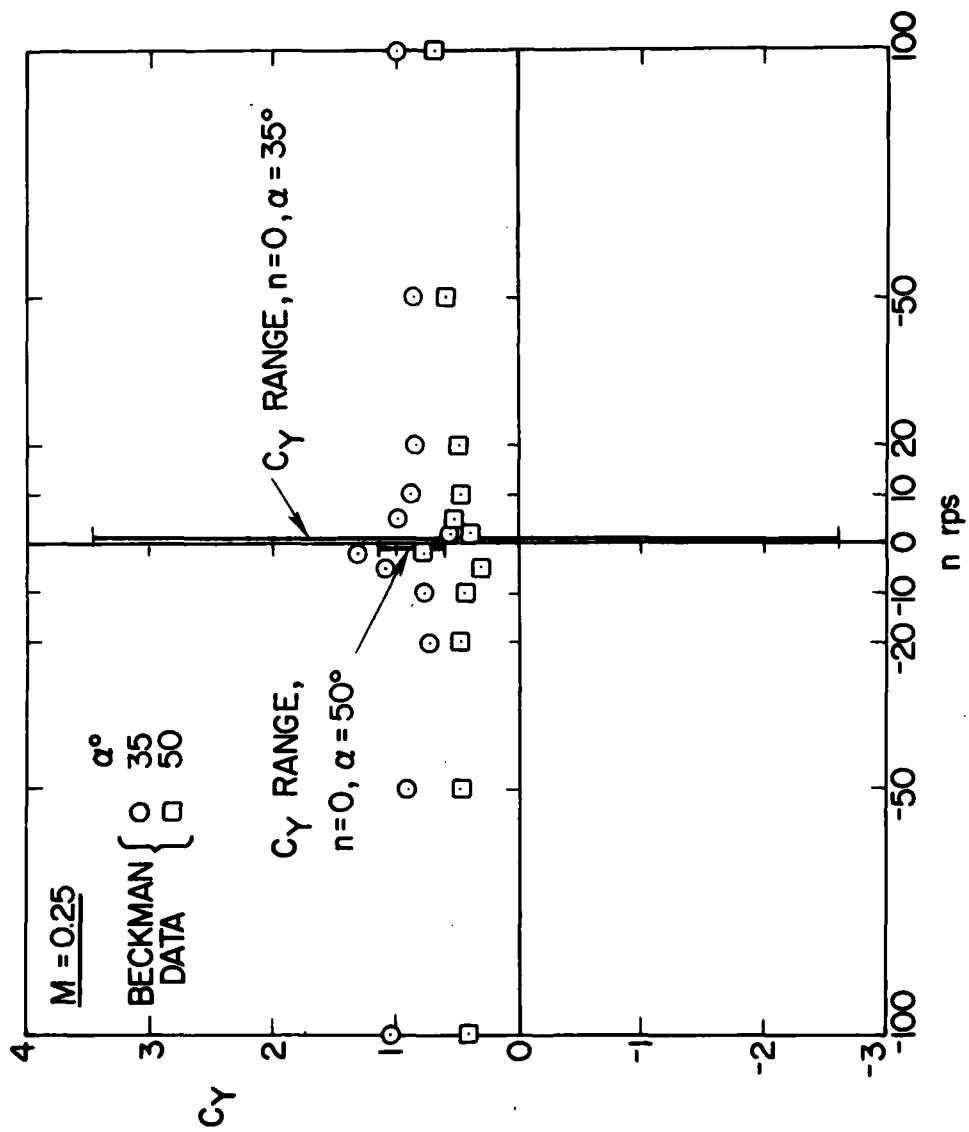


Figure 8. Concluded.



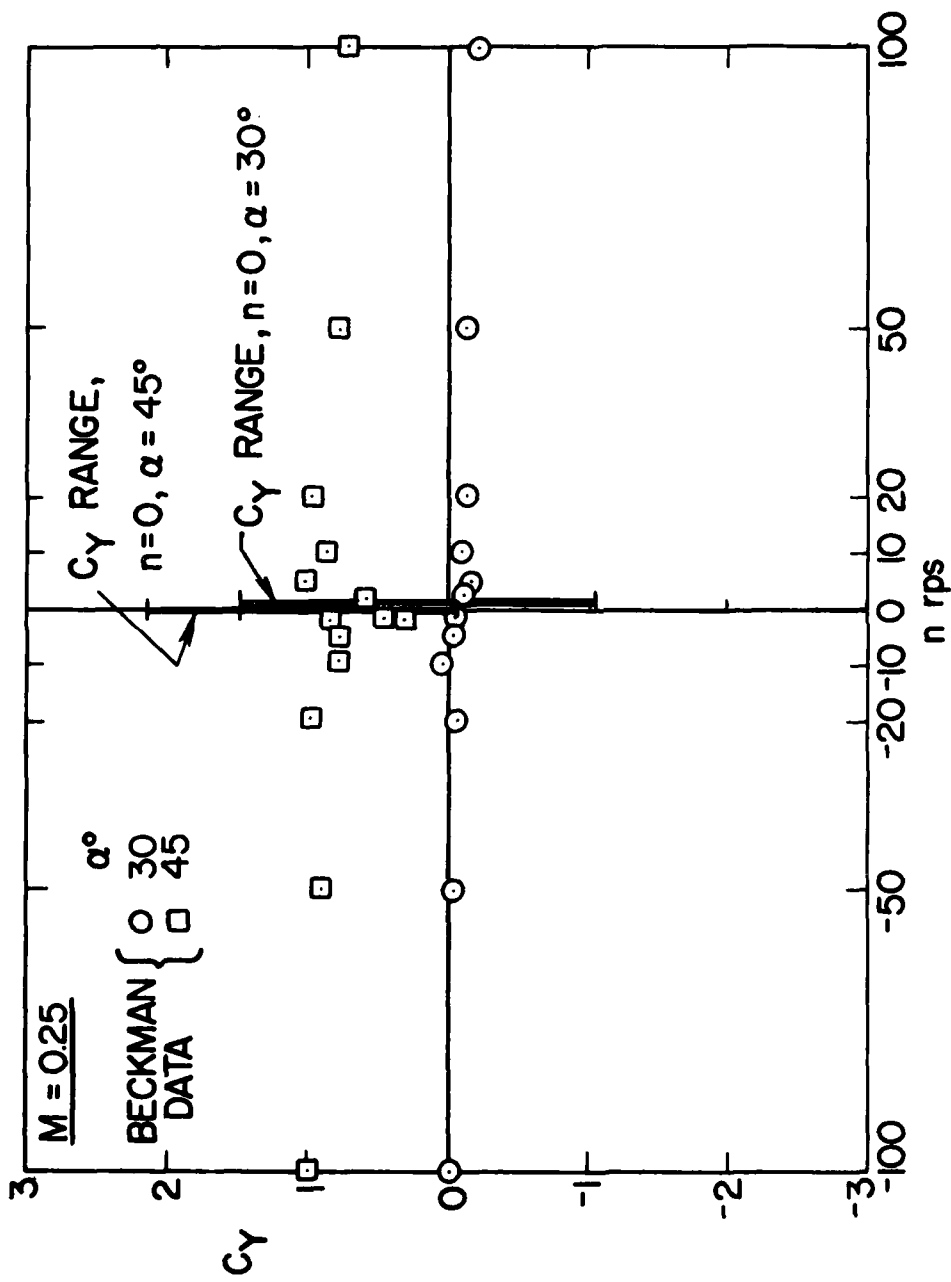
(a) Tip with 3 grit strips

Figure 9. Effect of tip spin on average side force



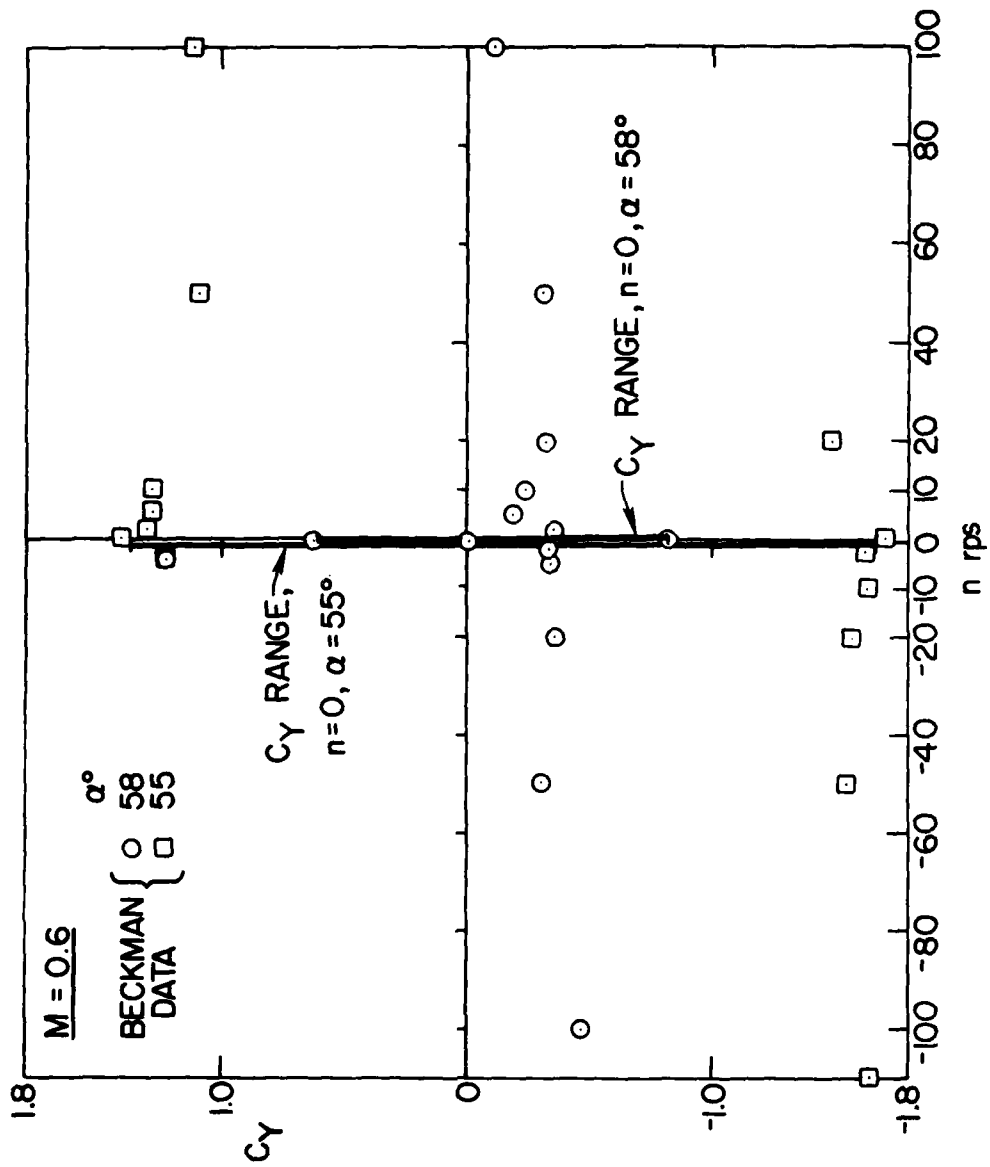
(b) Tip with 2 grit strips

Figure 9. Contined.



(c) Tip with 1 grit strip

Figure 9. Continued.



(d) Smooth tip
 Figure 9. Concluded.

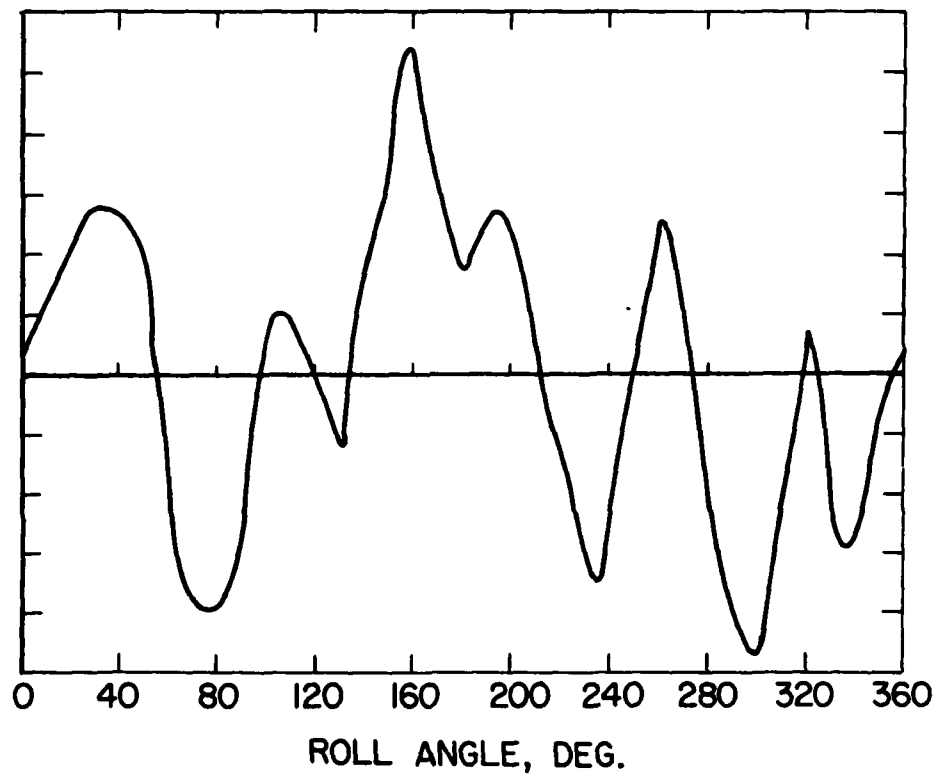


Figure 10a. Nose with 3 tape strips, +10 rps,
 $M = 0.25$, $\alpha = 50^\circ$.

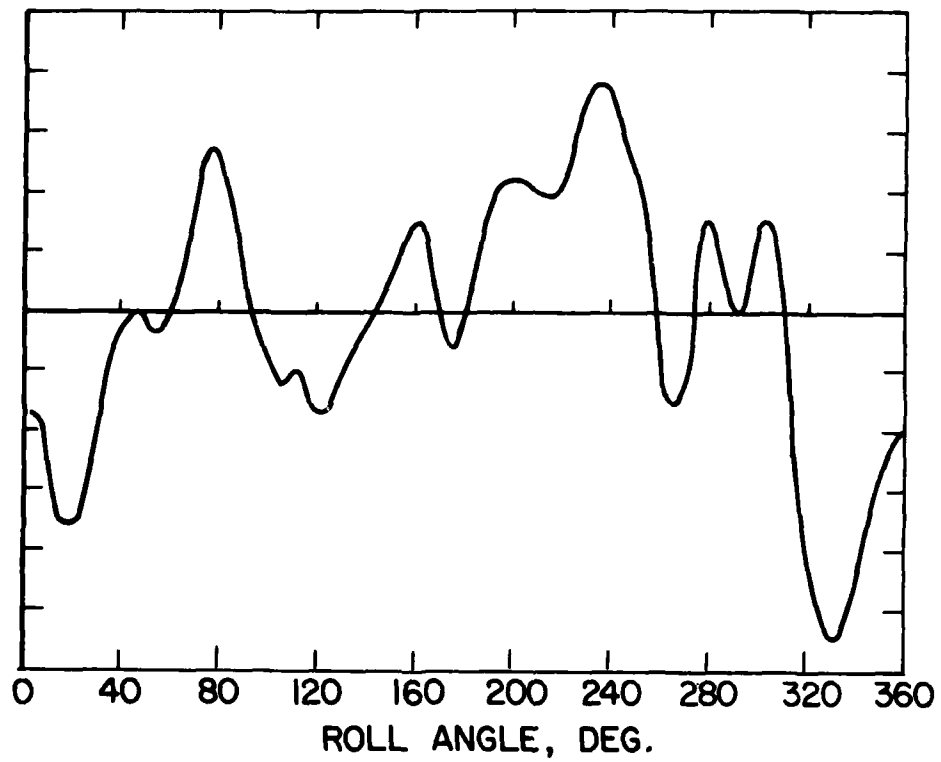


Figure 10b. Nose with 3 tape strips, +20 rps,
 $M = 0.25$, $\alpha = 50^\circ$.

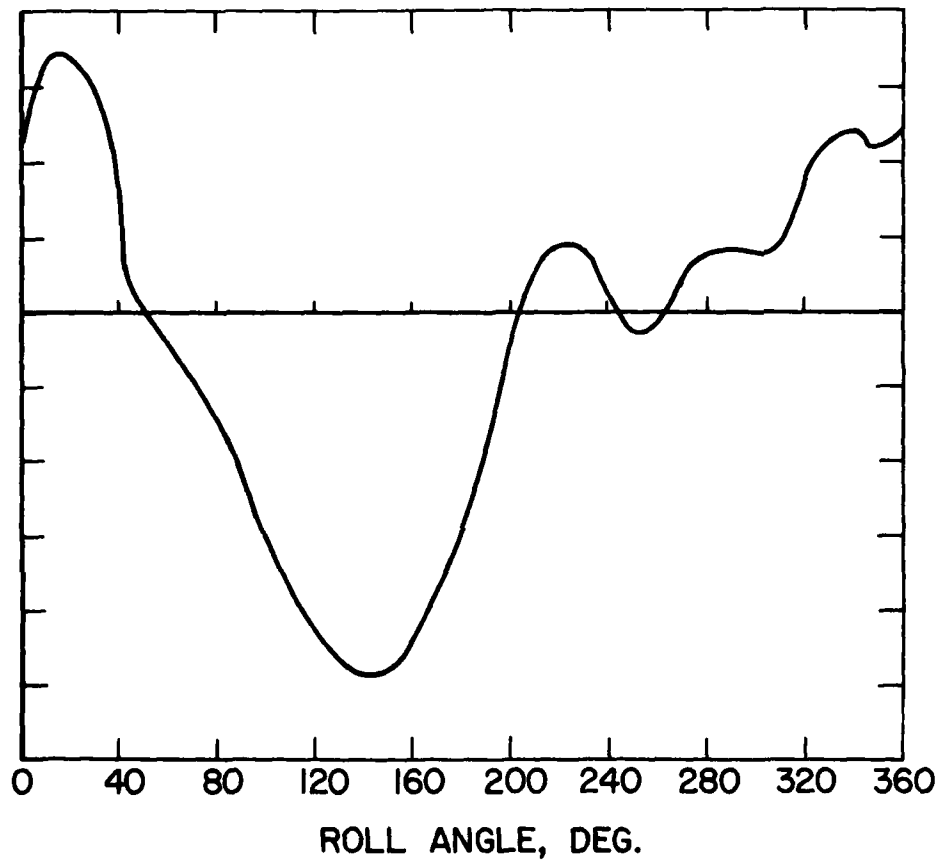


Figure 10c. Nose with 3 tape strips, +50 rps,
 $M = 0.25$, $\alpha = 50^\circ$.

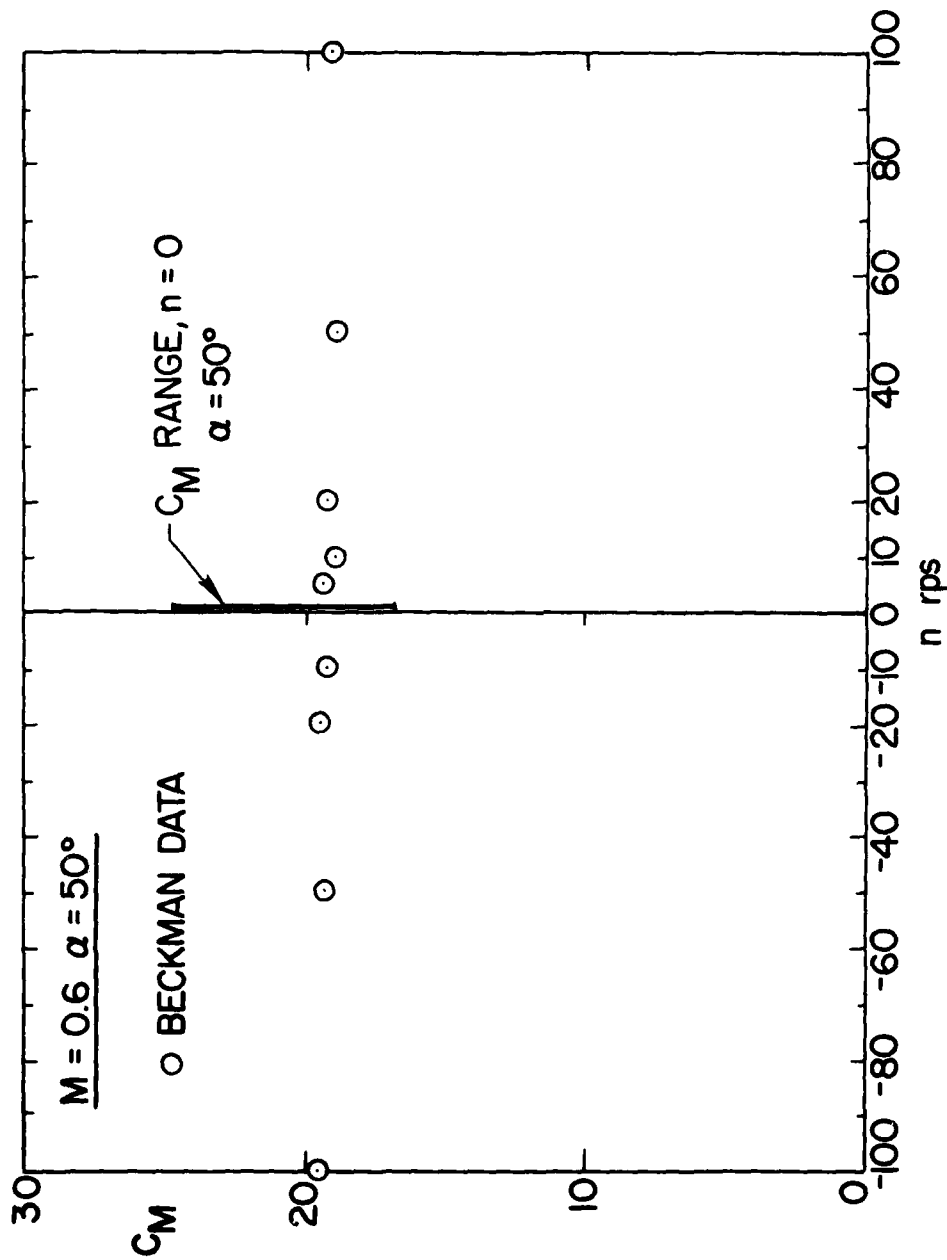


Figure 11. Effect on pitching moment of nosegrip with 3 grit strips.

LIST OF SYMBOLS

C_M	pitching moment coefficient
C_N	normal force coefficient
C_n	yawing moment coefficient
C_Y	side force coefficient
D	body diameter
M	Mach number
n	spin rate, rev/sec
α	angle of attack
ϕ	roll angle